State of the Global Climate 2023

WEATHER CLIMATE WATER

WORLD METEOROLOGICAL ORGANIZATION

WMO-No. 1347

WMO-No. 1347

Chair, Publications Board
World Meteorological Organization (WMO)
7 bis, avenue de la Paix
P.O. Box 2300
CH-1211 Geneva 2, Switzerland

Tel.: +41 (0) 22 730 84 03
Email: publications@wmo.int

ISBN 978-92-63-11347-4

Cover illustration: A melting glacier with chunks of ice breaking apart. The background captures the consequences of global warming on ice formations. Generative AI. Par Regina. N° de fichier: 640624130

Contents

We need your feedback

This year, the WMO team has launched a process to gather feedback on the State of the Climate reports and areas for improvement. Once you have finished reading the publication, we ask that you kindly give us your feedback by responding to this short survey. Your input is highly appreciated.

Key messages

2023 was the warmest year on record at 1.45 ± 0.12 °C above the pre-industrial average.

Concentrations of the three main greenhouse gases – carbon dioxide, methane and nitrous oxide – reached record-high observed levels in 2022. Real-time data show that levels continued to increase in 2023.

Ocean heat content reached its highest level in the 65-year observational record.

Global mean sea level reached a record high. The rate of sea-level rise in the past 10 years (2014–2023) has more than doubled since the first decade of the satellite record (1993–2002).

Antarctic sea-ice extent reached an absolute record low in February. The annual maximum extent was about 1 million km^2 below the previous record low maximum.

Preliminary data from the global set of reference glaciers for the hydrological year 2022–2023 show they experienced the largest loss of ice on record (1950–2023), driven by extremely negative mass balance in both western North America and Europe.

Glaciers in Switzerland have lost about 10% of their remaining volume in the past two years.

Extreme weather continued to lead to severe socioeconomic impacts. Extreme heat affected many parts of the world. Wildfires in Canada, Europe and Hawaii (United States of America) led to loss of life, the destruction of homes and large-scale air pollution. Flooding associated with extreme rainfall from Mediterranean Cyclone *Daniel* affected Greece, Bulgaria, Türkiye and Libya, with particularly heavy loss of life in Libya.

Food security, population displacement and impacts on vulnerable populations continued to be of mounting concern in 2023, with weather and climate hazards exacerbating the situation in many parts of the world.

Foreword

The climate crisis is the defining challenge that humanity faces.

The *WMO State of the Global Climate 2023* report confirms that the year 2023 broke every single climate indicator.

It was by far the warmest year on record. The global average temperature in 2023 was 1.45 ± 0.12 °C above the 1850–1900 average. Never have we been so close – albeit on a temporary basis – to the 1.5° C lower limit of the Paris Agreement on climate change.

Concentrations of greenhouse gases continued to rise. Ocean heat content and sea level reached record observed highs, and the rate of increase is accelerating. Antarctic sea-ice extent hit record observed lows. Key glaciers suffered record losses.

Heatwaves, floods, droughts, wildfires and intense tropical cyclones wreaked havoc on every continent and caused huge socioeconomic losses. There were particularly devastating consequences for vulnerable populations, who suffered disproportionate impacts.

Extreme climate conditions exacerbated humanitarian crises, with millions experiencing acute food insecurity and hundreds of thousands displaced from their homes.

WMO is committed to increasing collaboration with the international community to confront the enormity of this challenge.

WMO and its Members are expanding life-saving early warning services to achieve the ground-breaking Early Warnings for All initiative. A new Global Greenhouse Gas Watch (GGGW) seeks to provide scientifically based information for climate change mitigation. The transition to renewable energy must be supported by tailor-made weather and climate services.

To succeed, it is imperative to leverage efforts across the entire value chain – from improving climate data and monitoring to strengthening prediction and projections and building capacity. We must make climate information more accessible and actionable to serve society.

I hope this report will raise awareness of the vital need to scale up the urgency and ambition of climate action.

I take this opportunity to congratulate and thank the experts and lead authors who compiled this report. I extend my gratitude to all the contributors, particularly to WMO Member National Meteorological and Hydrological Services (NMHSs) and Regional Climate Centres (RCCs) and United Nations agencies.

(Prof. Celeste Saulo)
Secretary-General

Global climate indicators

Global climate indicators provide an overview of changes in the climate system.[1] The set of interlinked physical indicators presented here connect the changing composition of the atmosphere with changes in energy in the climate system and the response of land, ocean and ice.

Global climate indicators are based on a wide range of datasets that comprise data from multiple observing systems, including satellites and in situ networks (for details on the datasets used in the present publication, see Data set and methods).

Changes to the physical climate, measured in the present publication by key indicators, can have cascading impacts on national development and progress towards the United Nations Sustainable Development Goals (SDGs).[2] For example, changes in the acidity or temperature of the ocean can affect marine life, in turn potentially affecting coastal communities that may depend on the local catch for their livelihood or food security. Nevertheless, climate science has a critical role to play in facilitating sustainable development. As demonstrated by the United in Science 2023 report, weather-, climate- and water-related sciences support the achievement of many of the SDGs.[3] Recognizing the interconnections between climate and development can therefore lead to synergistic action – an increasing necessity as the world strays further from achieving both the SDGs and the Paris Agreement goals.[4]

BASELINES

Baselines are periods of time, usually spanning three decades or more, that are used as a fixed benchmark with which current conditions can be compared. For scientific, policy and practical reasons, several different baselines are used in the present publication, and these are specified in the text and figures. Where possible, the most recent WMO climatological standard normal, 1991–2020, is used for consistent reporting.

For some indicators, however, it is not possible to use the standard normal owing to a lack of measurements during the early part of the period. There are also two specific exceptions. First, for the global mean temperature time series – and only for the global mean series – a reference period of 1850–1900 is used. This is the baseline used by Working Group I in its contribution to the Sixth Assessment Report of the Intergovernmental Panel on Climate Change (IPCC AR6 WG I) as a reference period for pre-industrial conditions and is relevant for understanding progress in the context of the Paris Agreement. Secondly, greenhouse gas concentrations can be estimated much further back in time using gas bubbles trapped in ice cores. Therefore, the year 1750 is used in the present publication to represent pre-industrial greenhouse gas concentrations.

GREENHOUSE GASES

Concentrations of the three main greenhouse gases – carbon dioxide, methane and nitrous oxide – reached record-high observed levels in 2022, the latest year for which consolidated global values are available (1984–2022). Real-time data from specific locations show that levels of the three main greenhouse gases continued to increase in 2023.

Atmospheric concentrations of greenhouse gases reflect a balance among emissions from human activities, natural sources and sinks. Increasing levels of greenhouse gases in the atmosphere owing to human activities have been the major driver of climate change since the Industrial Revolution. Global average mole fractions of greenhouse gases – referred to in the present publication for simplicity as the "concentration" in the atmosphere – are calculated from in situ observations made at multiple sites through the Global Atmosphere Watch (GAW) Programme of WMO, and partner networks.

In 2022 – the latest year for which consolidated global figures are available – atmospheric levels of greenhouse gases reached new observed highs (see Figure 1), with globally averaged concentrations of carbon dioxide (CO_2) at 417.9 ± 0.2 parts per million (ppm), methane (CH_4) at 1 923 ± 2 parts per billion (ppb) and nitrous oxide (N_2O) at 335.8 ± 0.1 ppb, respectively 150%, 264% and 124% of pre-industrial (1750) levels. The rate of increase in CH_4 was the second highest on record, after 2021, and the rate of increase in N_2O was the highest on record. The rate of increase in CO_2 at 2.2 ppm was slightly below the 10-year average of 2.46 ppm yr^{-1}. CO_2 growth rate is typically lower in years that start with La Niña, as 2022 did, and higher in years that start with El Niño, as 2016 did.[5] Real-time data from specific locations, including Mauna Loa[6] (Hawaii, United States of America) and Kennaook/Cape Grim[7] (Tasmania, Australia) indicate that levels of CO_2, CH_4 and N_2O continued to increase in 2023.

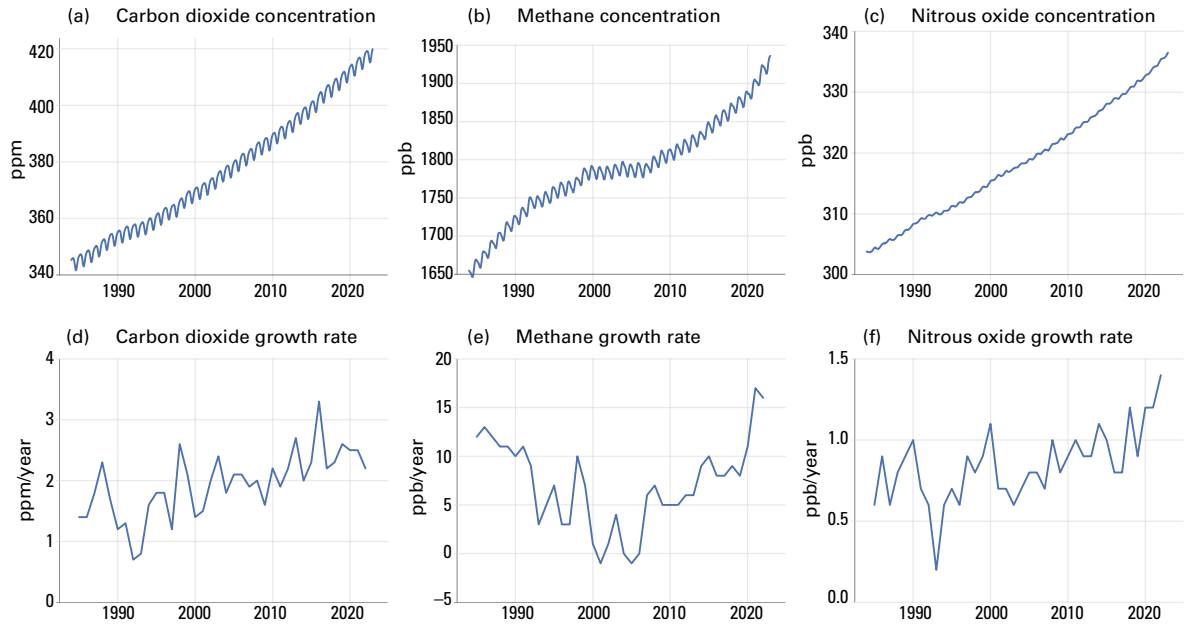

Figure 1. Top row: Monthly globally averaged mole fraction (measure of atmospheric concentration), from 1984 to 2022, of (a) CO_2 in ppm, (b) CH_4 in ppb and (c) N_2O in ppb. Bottom row: Growth rates representing increases in successive annual means of mole fractions for (d) CO_2 in ppm per year, (e) CH_4 in ppb per year and (f) N_2O in ppb per year.

Source: World Data Centre for Greenhouse Gases (WDCGG)

TEMPERATURE

The global mean near-surface temperature in 2023 was 1.45 ± 0.12 °C above the 1850–1900 average. 2023 was the warmest year in the 174-year observational record, clearly surpassing the previous joint warmest years, 2016 at 1.29 ± 0.12 °C above the 1850–1900 average and 2020 at 1.27 ± 0.13 °C.

The past nine years, 2015–2023, were the nine warmest years on record.

Record monthly global near-surface temperatures have been observed for the ocean – from April through December – and, starting slightly later, the land – from July through November.

The 10-year average 2014–2023 global temperature was 1.20 ± 0.12 °C above the 1850–1900 average, making it the warmest 10-year period on record.

Global mean near-surface temperature in 2023 was 1.45 ± 0.12 °C above the 1850–1900 average[8] (see Figure 2). The analysis is based on a synthesis of six global temperature datasets (see Data set and methods). 2023 was the warmest year in the 174-year instrumental record in each of the six datasets. The past nine years – from 2015 to 2023 – were the nine warmest years on record. The two previous warmest years were 2016, with an anomaly of 1.29 ± 0.12 °C, and 2020, with an anomaly of 1.27 ± 0.13 °C.

Globally, every month from June to December was record warm for the respective month. September 2023 was particularly noteworthy, surpassing the previous global record for September by a wide margin (0.46 °C–0.54 °C) in all datasets. The second-highest margin by which a September record was broken in the past 60 years (the period covered by all datasets) was substantially smaller, at 0.03 °C–0.17 °C in 1983. July is typically the warmest month of the year globally, and thus July 2023 became the warmest month on record.

The long-term increase in global temperature is due to increased concentrations of greenhouse gases in the atmosphere. The shift from La Niña, which lasted from mid-2020 to early 2023, to fully developed El Niño conditions by September 2023 (see Short-term climate drivers)

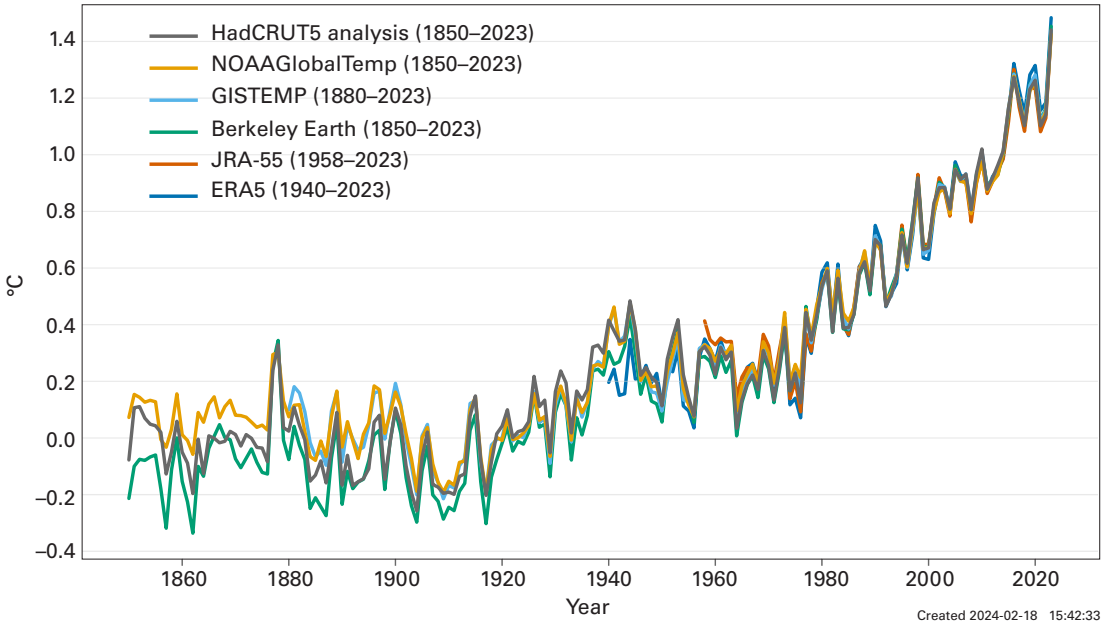

Figure 2. Annual global mean temperature anomalies (relative to 1850–1900)

Source: Data are from the six datasets indicated in the legend. See Data set and methods for details.

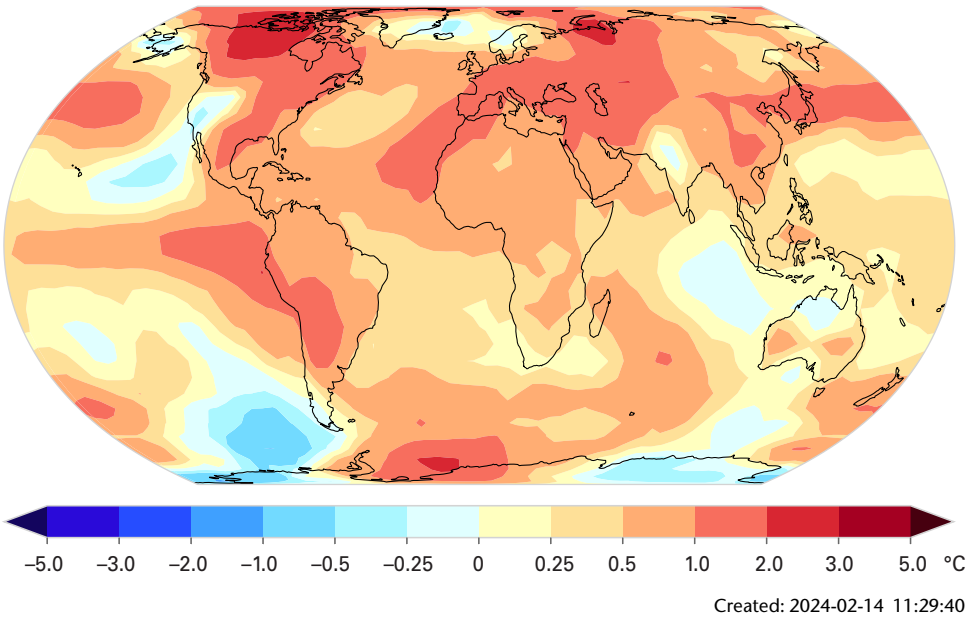

Figure 3. Mean near-surface temperature anomalies (difference from the 1991–2020 average) for 2023.

Source: Data are the median of the six datasets indicated in the legend. See Data set and methods for more details

likely explains some of the rise in temperature from 2022 to 2023. However, some areas of unusual warming, such as the North-East Atlantic (see Figure 3) do not correspond to typical patterns of warming or cooling associated with El Niño. Other factors, which are still being investigated, may also have contributed to the exceptional warming from 2022 to 2023, which is unlikely to be due to internal variability alone.[9]

The average global temperature over the past 10 years, from 2014 to 2023, was 1.20 ± 0.12 °C above the 1850–1900 average, making the past 10 years the warmest among all 10-year periods on record in all six datasets.

Between late spring in the northern hemisphere and the end of 2023, global average sea-surface temperatures (SSTs) were also at a record observed high. The records for July, August and September were each broken by a large margin (between 0.21 °C and 0.27 °C). Exceptional warmth relative to the 1991–2020 baseline was recorded in the eastern North Atlantic, the Gulf of Mexico and the Caribbean, the North Pacific extending eastward from the Sea of Japan, the Arabian Sea and large areas of the Southern Ocean (see Figure 3; see also Marine heatwaves and cold spells).

Observed global land temperature anomalies reached record levels in July and August, somewhat later than for SSTs, but the September average was also a record by a large margin of 0.53 °C–0.71 °C. The second-widest margin by which a record has been broken in the past 60 years was 0.22 °C–0.27 °C in September 2002. In 2023, most land areas were warmer than the 1991–2020 average (see Figure 3). Unusual warmth was reported across large areas of northern Canada, the southern United States of America, Mexico and Central America, as well as large areas of South America. Large areas from Central Asia to western Europe, including parts of North Africa and the Arabian Peninsula, were also unusually warm, as were South-East Asia and Japan.

OCEAN

Increasing human emissions of carbon dioxide (CO_2) and other greenhouse gases cause a positive radiative imbalance at the top of the atmosphere. This imbalance leads to the accumulation of energy in the Earth system in the form of heat, which is driving global warming.[10,11] The ocean, which covers about 70% of the Earth's surface, absorbs heat and CO_2, which can act to slow the rate of warming in the atmosphere. However, the heat absorbed by the ocean leads to ocean warming, which, together with the melting of ice on land, raises sea levels, while the absorption of CO_2 leads to ocean acidification. Warming waters, sea-level rise and ocean acidification all have significant effects on the ocean, as well as on the plants and animals that live in it and the people who rely upon it for their livelihoods.

OCEAN HEAT CONTENT

In 2023, ocean heat content reached its highest level in the 65-year observational record.

About 90% of the energy that has accumulated in the Earth system since 1971 is stored in the ocean. As energy has accumulated in the ocean, it has warmed, and global ocean heat content has increased (see Figure 4).

According to a consolidated analysis based on several individual datasets, the upper 2 000 m of the ocean continued to warm in 2023.[12] Ilt is expected that warming will continue – a change that is irreversible on centennial to millennial timescales.[13,14] Ocean heat content in 2023 was the highest on record, exceeding the 2022 value by 13 ± 9 ZJ (see Figure 4)[15] cconsistent with estimates published in early 2024.[16]

All datasets agree that ocean warming rates show a particularly strong increase in the past two decades. The rate of ocean warming for the 0–2 000 m layer was 0.7 ± 0.1 W m^{-2} from 1971 to 2023 on average, but 1.0 ± 0.1 W m^{-2} from 2005 to 2023 (the period covered by the Argo programme). The steady increase in ocean warming rates[17,18] is seen consistently in direct estimates from in situ observations, indirect estimates from remote sensing and direct estimates of the net flux at the top of the atmosphere as measured by satellites.[19] Different drivers of this change are discussed in literature, including a change in anthropogenic climate forcing[20] and natural variability.[21] Deep-ocean global warming below 2 000 m depth is estimated to be 0.07 ± 0.03 W m^{-2} from 1992 to 2022.[22]

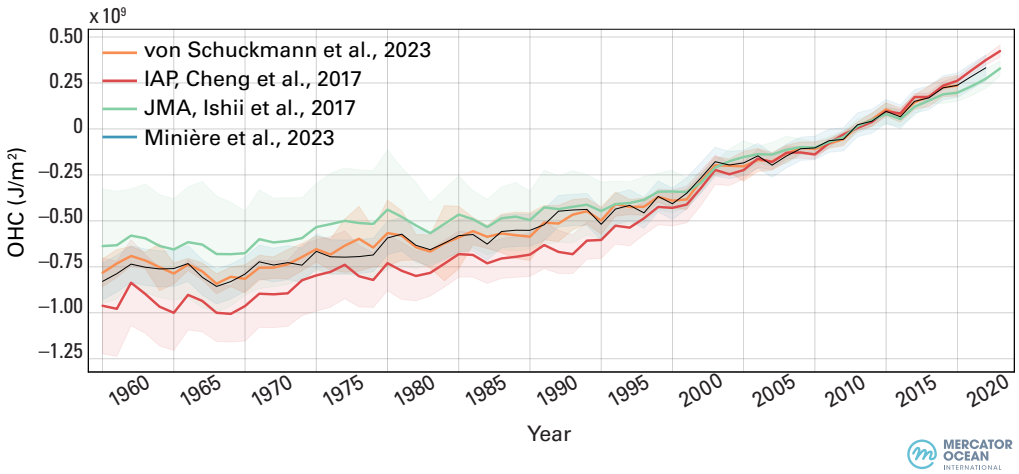

Figure 4. Global ocean heat content anomalies relative to the 2005–2021 average for the 0–2 000 m depth layer 1960–2023 (orange). Ensemble mean time series and ensemble standard deviation (2-standard deviations, shaded) updated from Schuckmann et al., 2023 (red); Cheng et al., 2017 (green); Minière et al., 2023 (light blue); and Ishii et al., 2017 (dark blue).

Source: Mercator Ocean international.

Although ocean heat content has increased strongly through the entire water column, the rate of warming has not been the same everywhere.[23] The strongest warming in the upper 2 000 m occurred in the Southern Ocean (60° S–35° S), North Atlantic (20° N–50° N) and South Atlantic (60° S–0° S) (see Figure 5). The Southern Ocean domain is the largest reservoir of heat, accounting for about 32% of the global ocean heat content increase in the upper 2 000 m since 1958.[24] The Atlantic Ocean accounts for approximately 31% of the global 0–2 000 m ocean heat content increase, and the Pacific Ocean for about 26%.

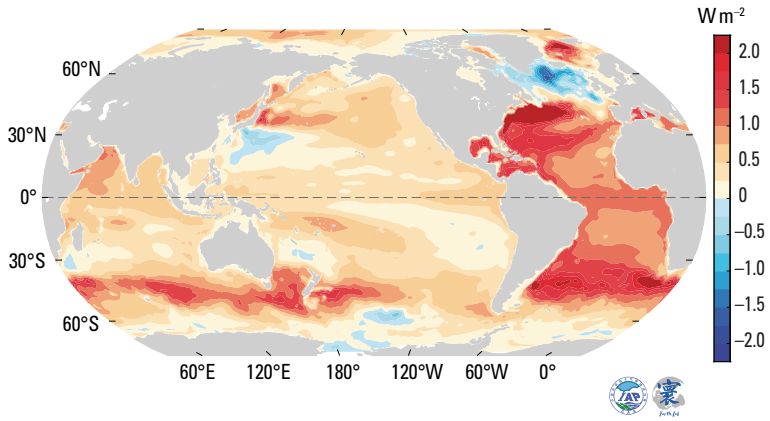

Figure 5. Observed upper 2000 m OHC trend from 1958 to 2023.

Source: Data updated from Cheng et al.[25]

Some relatively small regions are cooling, including the subpolar North Atlantic Ocean, extending from near the surface to a depth of over 800 m (also the only area to show centennial cooling at the surface). The contrasting pattern of cooling (50° N–70° N) and warming (20° N–50° N) in the North Atlantic has been associated with a slowing of the Atlantic Meridional Overturning Circulation and local interactions between the air and sea.[26] Other cooling regions include the North-West Pacific, the South-West Pacific and the South-West Indian Ocean.

SEA LEVEL

In 2023, global mean sea level reached a record high in the satellite record (from 1993 to present), reflecting continued ocean warming as well as the melting of glaciers and ice sheets

The rate of global mean sea-level rise in the past 10 years (2014–2023) is more than twice the rate of sea-level rise in the first decade of the satellite record (1993–2002).

Global mean sea level (GMSL) continued to rise in 2023 (see Figure 6). The La Niña conditions between mid-2020 and early 2023 had only a small apparent effect on GMSL, unlike the 2011 La Niña, which led to a temporary decrease in GMSL of several millimetres. The rapid rise observed in 2023 is likely due in part to El Niño. The long-term rate of sea-level rise has more than doubled since the start of the satellite record, increasing from 2.13 mm yr^{-1} between 1993 and 2002 to 4.77 mm yr^{-1} between 2014 and 2023.

From January to March 2023, sea levels (see Figure 7) were higher than the long-term average (1993–2012) in the western tropical Pacific. This is characteristic of warm seawater in the region associated with El Niño–Southern Oscillation (ENSO)-neutral conditions. Sea levels in the North Atlantic and eastern tropical Pacific were lower than the long-term average. Warming of the surface waters in the eastern tropical Pacific during

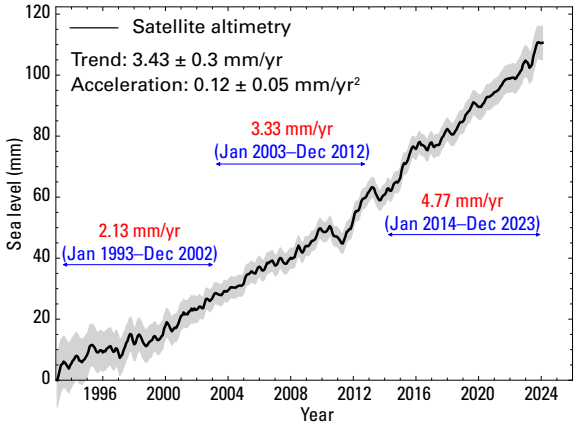

Figure 6. GMSL evolution between January 1993 and December 2023 based on satellite altimetry. The black line is the best estimate, and the grey shaded area indicates uncertainty. Red and blue annotations indicate the average rate of sea-level rise during three decades of the record as indicated.

Source: AVISO altimetry

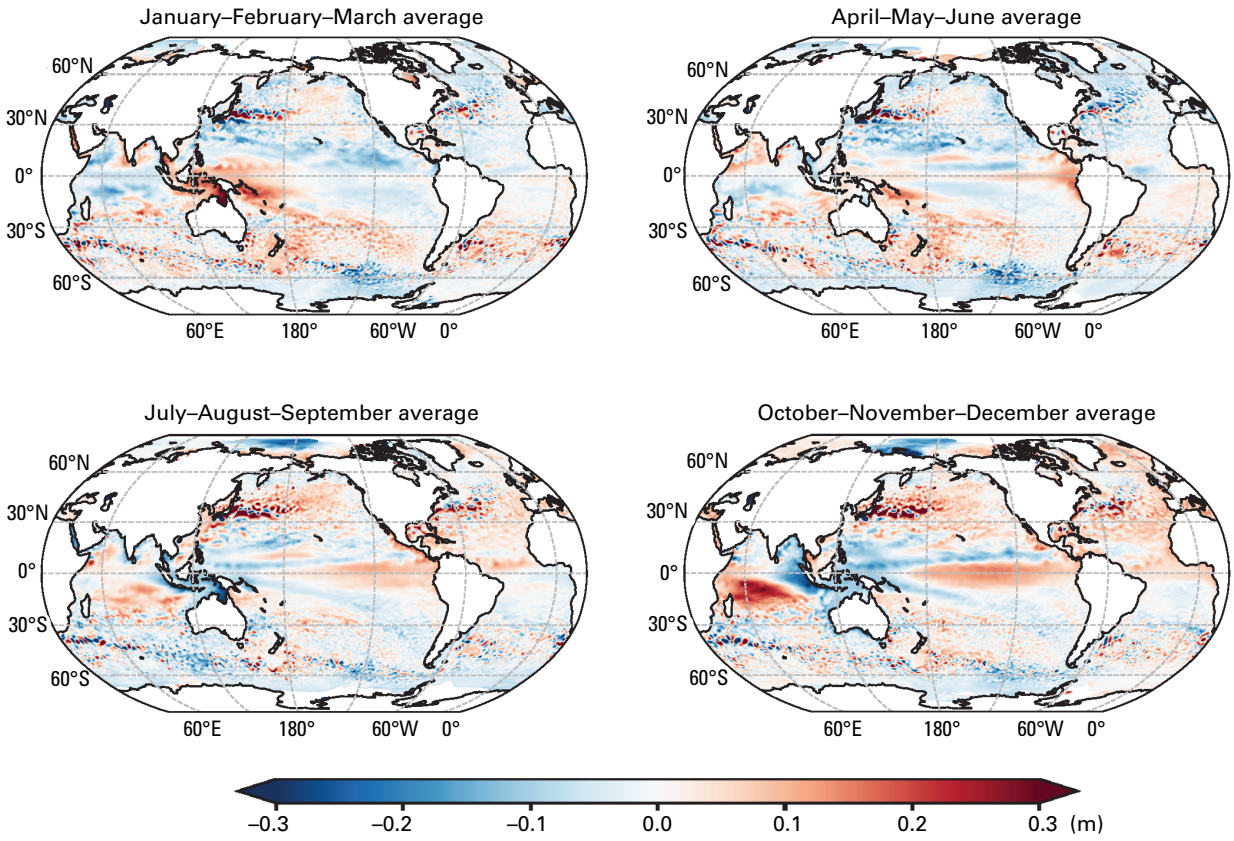

Figure 7. Three-month averages of altimetry-based sea-level anomalies (relative to the 1993–2012 average, which is the product climatology) for (top left) January–March 2023, (top right) April–June 2023, (bottom left) July–September 2023 and (bottom right) October–December 2023

Source: Data downloaded from the Copernicus Marine Service

the early stages of the 2023 El Niño (see Short-term climate drivers) led to an increase in sea levels relative to the long-term mean in the most eastern part of the tropical Pacific between April and June. Between July and September, the El Niño signature was clearly visible, with above-average sea levels from the mid-tropical Pacific to the coasts of Central and South America. Above-average sea levels were also observed in the tropical and North-East Atlantic, associated with the anomalous warming in these areas during the northern hemisphere summer. From October to the end of the year, the El Niño pattern continued to develop. The shift to the positive phase of the Indian Ocean Dipole (IOD) led to higher-than-average sea levels in the western Indian Ocean and lower-than-average sea levels in the East (see Short-term climate drivers).

MARINE HEATWAVES AND COLD SPELLS

As with heatwaves and cold spells on land, marine heatwaves and cold spells are prolonged periods of extreme high or low temperatures in the seas and ocean that can have a range of consequences for marine life and dependent communities.[27] Marine heatwaves have become more frequent, intense and longer lasting since the late twentieth century, while marine cold spells have been decreasing by those same measures. Satellite retrievals of sea-surface temperature (SST) are used to monitor marine heatwaves and cold spells globally, categorized in the present publication as "moderate", "strong", "severe", "extreme" or "ice" (for definitions, see Data set and methods).

El Niño events tend to cause widespread marine heatwaves in the eastern tropical Pacific. While this region did experience strong marine heatwaves in 2023 until late October (see Figure 8a), and moderate marine heatwaves for the rest of 2023, the overall areal coverage was smaller than in previous El Niño events.

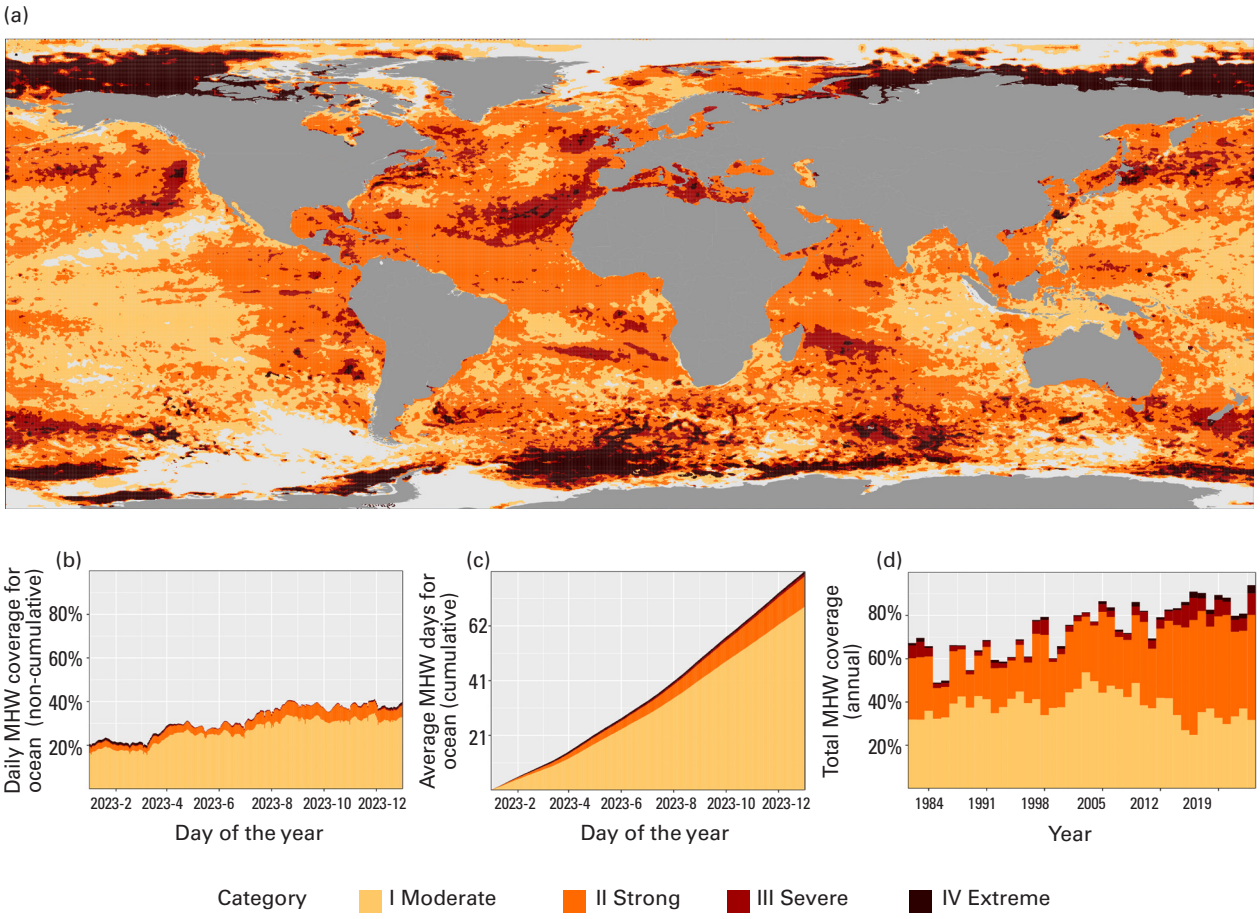

Figure 8. (a) Global map showing the highest marine heatwave category (for definitions, see Data set and methods) experienced at each pixel over 2023 (reference period 1982–2011). Light grey indicates that no marine heatwave occurred in a pixel over the entire year; (b) Stacked bar plot showing the percentage of the surface of the ocean experiencing a marine heatwave on any given day of the year; (c) Stacked bar plot showing the cumulative number of marine heatwave days averaged over the surface of the ocean, calculated by dividing the cumulative sum of marine heatwave days per pixel weighted by the surface area of those pixels); and (d) Stacked bar plot showing the total percentage of the surface of the ocean that experienced a marine heatwave from 1982 to present. Data are from the National Oceanic and Atmospheric Administration (NOAA) Optimum Interpolation Sea-Surface Temperature (OISST).

Source: Robert Schlegel

Of note in 2023 were the persistent and widespread marine heatwaves in the North Atlantic, which began in the northern hemisphere spring, peaked in extent in September and persisted through the end of the year. While areal coverage diminished in December, intensity increased. The end of 2023 saw a broad band of severe and extreme marine heatwaves across the North Atlantic, with temperature anomalies in the open ocean of +3 °C.

The Mediterranean Sea was also unusually warm relative to the baseline period and experienced near-complete coverage of strong and severe marine heatwaves for the twelfth consecutive year. In the southern hemisphere, the waters surrounding New Zealand remained 1 °C–2 °C above the long-term average from January to September (~270 days).

At the end of 2023, most of the global ocean from roughly 20° N to 20° S of the equator had been in a marine heatwave state since early November. In contrast, there were almost no occurrences of marine cold spells within 60° N or 60° S of the equator in 2023 (see Figure 9a).

The global ocean experienced an average daily marine heatwave coverage of 32% (see Figure 8b), well above the previous record of 23% in 2016. In contrast, the average daily coverage of marine cold spells (see Figure 9b) was only 4%, far below 2022 (7%).

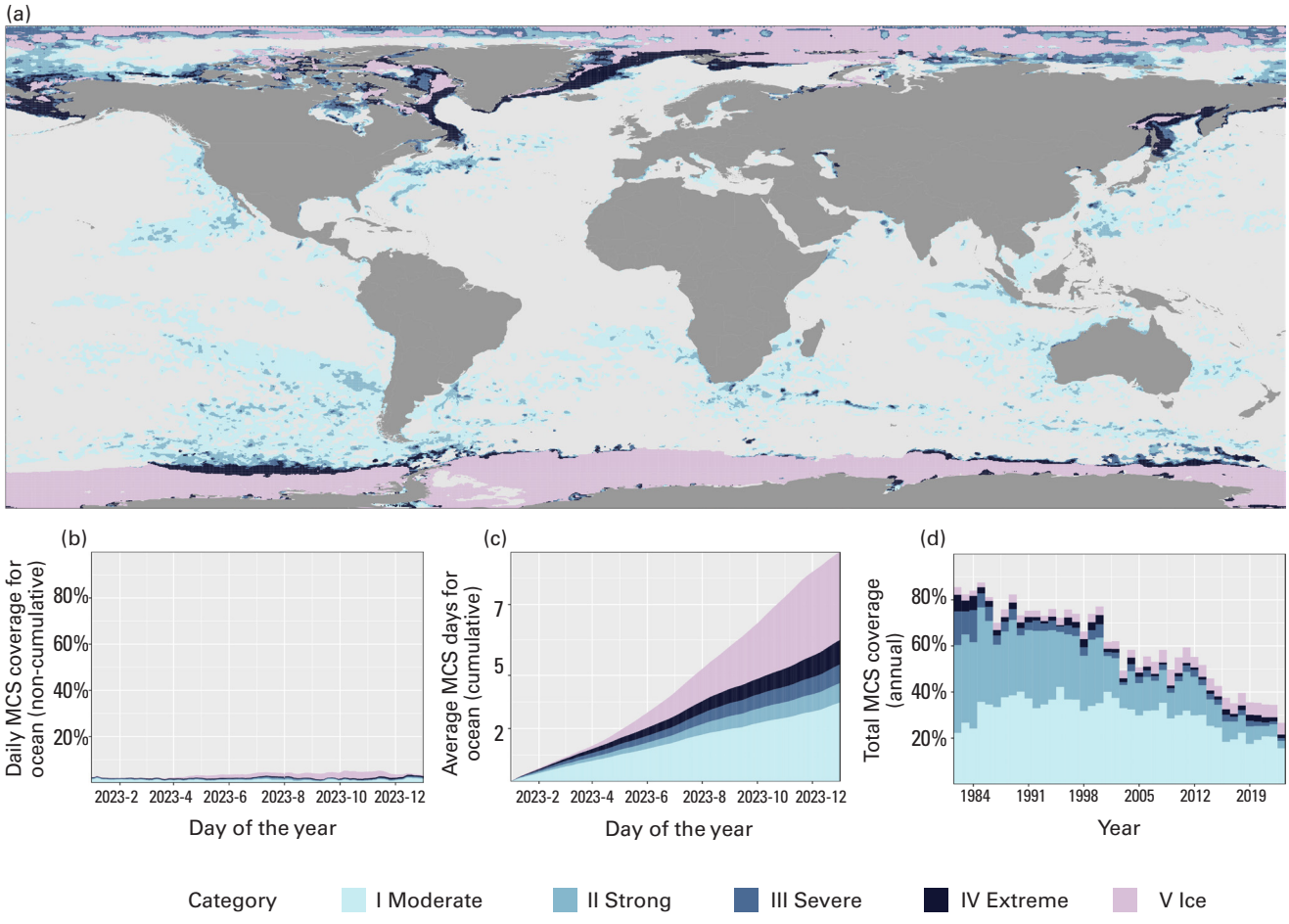

Figure 9. As for Figure 8 but showing marine cold spells rather than heatwaves. Data are from the NOAA OISST.

Source: Robert Schlegel.

OCEAN ACIDIFICATION

The ocean absorbs about one quarter of the annual emissions of anthropogenic carbon dioxide (CO_2) released into the atmosphere.[28,29] CO_2 reacts with seawater and alters the carbonate chemistry, resulting in a decrease in pH referred to as "ocean acidification" (see Figure 10). Ocean acidification affects organisms and ecosystem services, including food security, by reducing biodiversity, degrading habitats and endangering fisheries and aquaculture.[30] The Sixth Assessment Report of the Intergovernmental Panel on Climate Change (IPCC AR6) concluded that "[t]here is very high confidence that present-day surface pH values are unprecedented for at least 26 000 years and current rates of pH change are unprecedented since at least that time".[31]

Although global efforts, many supported by the Intergovernmental Oceanographic Commission (IOC) of the United Nations Educational, Scientific and Cultural Organization (UNESCO), and led by the Global Ocean Acidification Observing Network (GOA-ON) and the United Nations Ocean Decade-endorsed Ocean Acidification Research for Sustainability (OARS) Programme, have resulted in an increase in the number of ocean acidification observations, many regions remain under sampled. Data collected for Sustainable Development Goal (SDG) Indicator 14.3.1 (Average marine acidity (pH) measured at agreed suite of representative sampling stations) show that current coverage is inadequate (see Figure 11), with time series not long enough to determine trends and gaps in observations in all areas. Global trends illustrating the decrease in global ocean surface pH (see Figure 10) show the large-scale effects of CO_2 emissions. However, the rate of change in ocean acidification, and its pattern and scale, show great regional and temporal variability, and understanding these variations requires high-resolution, long-term observation at scales relevant to the affected communities.

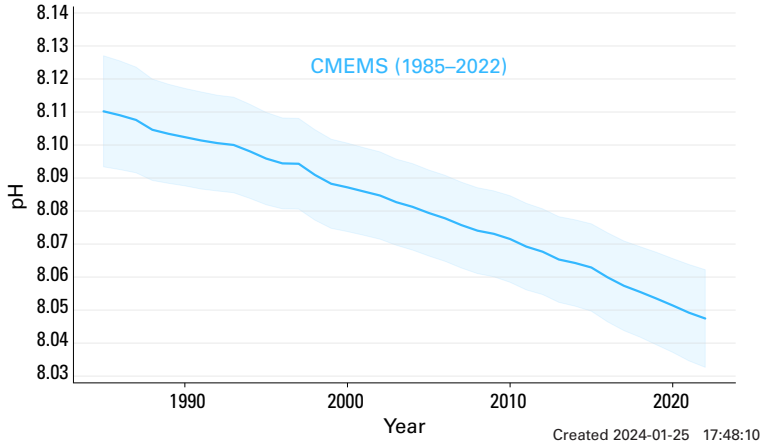

Figure 10. Global annual mean ocean surface pH (purple) covering the period 1985–2022. The shaded area indicates the estimated uncertainty in the values.

Source: Data from the Copernicus Marine Environment Monitoring Service.

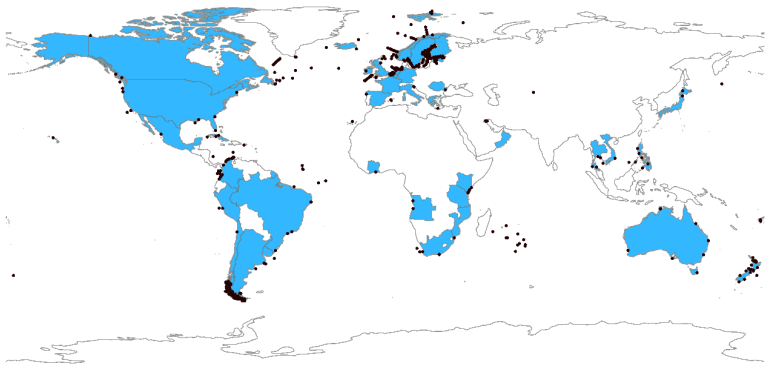

Figure 11. Map illustrating surface ocean carbonate chemistry measurement locations received for SDG Indicator 14.3.1 (Average marine acidity (pH) measured at agreed suite of representative sampling stations) ocean acidification reporting by IOC/UNESCO. Countries highlighted in light blue reported data in accordance with the SDG Indicator 14.3.1 methodology. Black dots show the location of sampling stations from which data were collected.

Source: IOC/UNESCO

CRYOSPHERE

The cryosphere comprises the frozen parts of Earth, namely glaciers and ice sheets, sea ice, snow and permafrost. The inhospitable and often remote environments in which ice forms mean that it has sometimes been challenging to undertake long-term measurements of the cryosphere. At the same time, the profound changes seen in the cryosphere clearly illustrate the global scale of climate change.

SEA-ICE

Arctic sea-ice extent remained well below normal in 2023, with the annual maximum and annual minimum extents being respectively the fifth and sixth lowest in the 45-year satellite record.

Antarctic sea-ice extent reached an absolute record low for the satellite era (from 1979 to present) in February. Sea-ice extent was at a record low for the time of year from June until early November, and the annual maximum in September was about 1 million km^2 below the previous record low maximum.

Arctic sea-ice extent reached its annual maximum of 14.62 million km^2 on 6 March, the fifth lowest in the satellite record.[32] The annual minimum Arctic sea-ice extent was reached on 19 September (see Figure 12, left),[33] with a minimum extent of 4.23 million km^2, well below the long-term average (1991–2020) of ~5.5 million km^2. This was the sixth lowest minimum Arctic sea-ice extent in the satellite record (1979–2023), not as extreme as 2012 or 2020 but only slightly higher than 2007, 2016 and 2019, and continuing the long-term trend of reduced late-summer and early-autumn Arctic ice cover. Major negative anomalies were observed in the Beaufort, Chukchi and East Siberian Seas (see Figure 12, right). The year ended with extents close to the long-term average, but still the ninth lowest in the satellite record.[34]

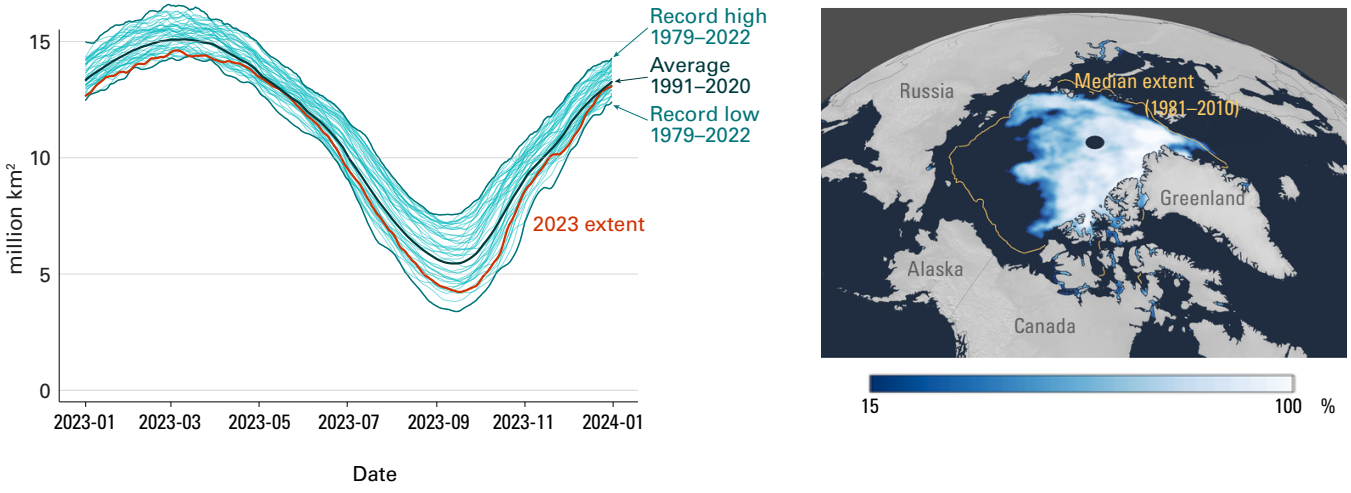

Figure 12. (left) Daily Arctic sea-ice extent from January through December, showing 2023 (red line) against the climate normal (1991–2020, dark blue), and the record highest and lowest extents for each day (mid-blue). Individual years are shown in light blue. (right) Sea-ice concentration on 19 September 2023, at the annual minimum Arctic sea-ice extent. The yellow line indicates the median ice edge for the 1981–2010 period.[35]

Source: Data and map from the National Snow and Ice Data Center (NSIDC).

Antarctic sea-ice extent had declined to 1.79 million km² on 21 February 2023 (see Figure 13, left), an all-time minimum for the satellite era (from 1979 to present) and slightly less than the previous record low, which was set in 2022.[36] Sea-ice extent remained below the average as the growth season commenced, reaching a record low for the time of year in May. Slow growth continued with exceptional record low extents between July and the annual maximum, likely in association with the warming of the Southern Ocean.[37] The maximum Antarctic sea-ice extent for 2023 (see Figure 13, right) was 16.96 million km² on 10 September, roughly 1.5 million km² below the 1991–2020 average and 1 million km² below the previous record low maximum set in 1986.[38] Record low sea-ice extents for the time of year continued until early November, but a slower-than-average rate of decline in December brought sea-ice extents closer to the long-term mean by the end of the year.[39]

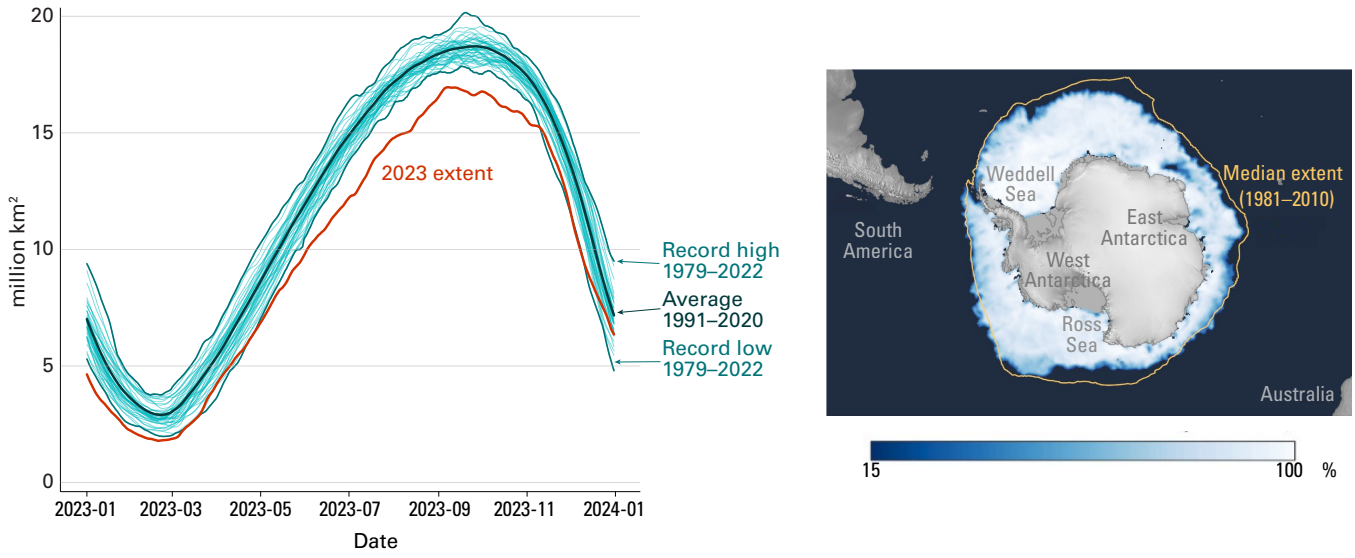

Figure 13. (left) Daily Antarctic sea-ice extent from January through December, showing 2023 (red line) conditions against the 1991–2020 climate normal (dark blue), and the record highest and lowest extents for each day (mid-blue). Individual years are shown in light blue. (right) Sea-ice concentration on 10 September 2023, at the 2023 annual maximum extent. The yellow line shows the median ice edge for the 1981–2010 climatology period.[40]

Source: Data and map from NSIDC.

ICE SHEETS

It was the warmest summer on record at Summit Station, 3.4 °C warmer than the 1991–2020 average and 1.0 °C warmer than the previous record.

An ice sheet[41] is an expanse of ice originating on land that covers an area of more than 50 000 km². There are two principal ice sheets in the present-day climate system, one in Greenland and one in Antarctica.[42] The total mass balance of an ice sheet is the sum of three components: surface mass balance, marine mass balance and basal mass balance. Surface mass balance is the difference between snow accumulation and meltwater runoff from the ice sheet. Marine mass balance is the mass loss at the edge of the ice sheet from the calving of icebergs and the melting of ice that is in contact with the ocean. Basal mass balance consists of melting at the ice sheet bed owing to geothermal heat and friction as the ice slides over the ground beneath. A negative mass balance indicates loss of ice mass; a positive mass balance indicates gain.

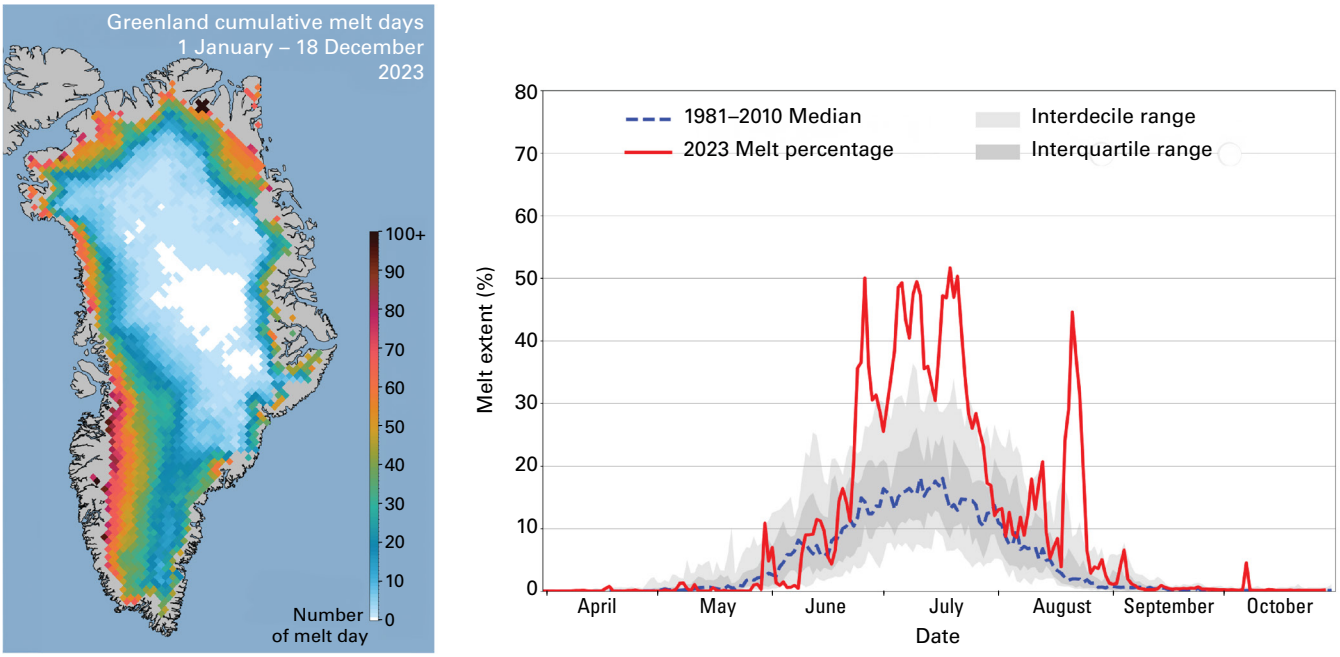

Figure 14. Greenland ice sheet melt conditions through 2023: (left) Cumulative melt days for Greenland in 2023. White areas indicate no melting occurred. (right) Percentage of the ice sheet experiencing melting conditions each day.

Source: Images and analysis courtesy of Thomas Mote, University of Georgia, and the National Snow and Ice Data Center (NSIDC).

Based on estimates from an ensemble of regional climate models, the Greenland ice sheet continued to lose mass in the hydrological year 2022/2023 (from 1 September 2022 to 31 August 2023).[43] Annual snow accumulation over Greenland still exceeds surface melt in most years, giving a positive surface mass balance. For 2022–2023 this was estimated at +317 Gt, below the long-term average but well above the extreme melt years of 2011–2012 and 2018–2019. Combined with the basal mass balance (–27 Gt) and the marine mass balance (–504 Gt), the estimated 2022–2023 ice sheet total mass balance was about –217 Gt.

The summer 2023 melt season was relatively intense, punctuated by major heatwaves in July and August.[44] Satellite melt extent data indicate that the ice sheet had the third highest cumulative melt-day area[45] on record (1978–2023), after the extreme melt season of 2012 and 2010 (see Figure 14). It was the warmest summer on record (1987–present) at Summit Station,[46] 3.4 °C warmer than the 1991–2020 average and 1.0 °C warmer than the previous record.[47] Summit Station experienced melting conditions for the fifth year on record (2012, 2019, 2021, 2022 and 2023); ice core records indicate that significant melting conditions last happened in the late nineteenth century.[48]

The Ice Sheet Mass Balance Inter-comparison Exercise has documented the acceleration in combined mass loss from the Greenland and Antarctic ice sheets over the period of the satellite record, 1992–2020.[49] The average total mass balance of the Greenland and Antarctic ice sheets over this period were –169 Gt yr^{-1} and –92 Gt yr^{-1},[50] respectively, and –261 Gt yr^{-1} combined. Combining the two ice sheets, the seven highest melt years on record have all occurred since 2010, and average rates of mass loss increased from 105 Gt yr^{-1} between 1992 and 1996 to 372 Gt yr^{-1} between 2016 and 2020. This is equivalent to ~1 mm yr^{-1} of global sea-level rise attributable to the polar ice sheets in the latter period.

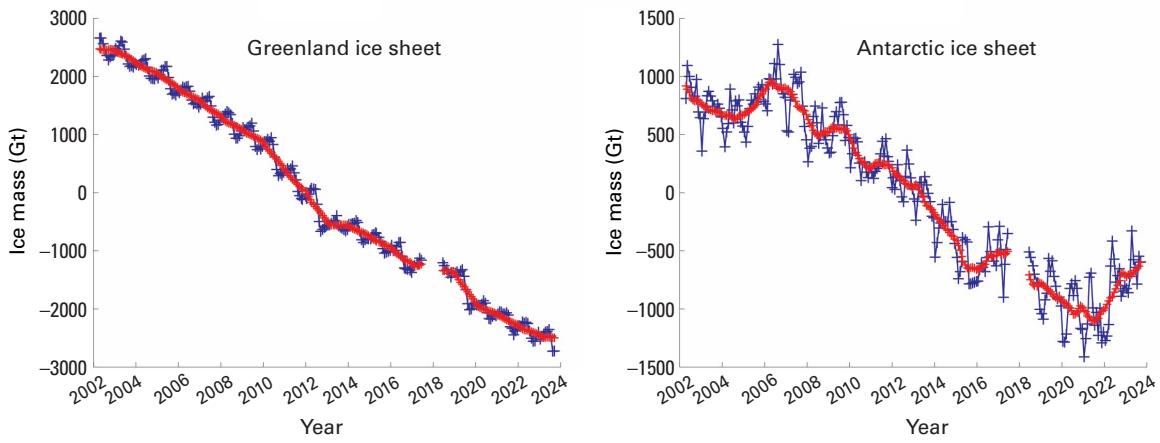

Figure 15. Gravitational mass balance data from the GRACE satellite mission for the Greenland and Antarctic ice sheets, from April 2002 through September 2023.

Source: Data and analysis courtesy of Isabella Velicogna.

Data and modelled estimates of mass balance from 2023 are consistent with these recent rates of mass loss in Greenland, but the Antarctic ice sheet gained mass owing to higher-than-normal snow accumulation in the past year and a half (see Figure 15). Gravitational mass balance data from the Gravity Recovery and Climate Experiment (GRACE) satellite mission for the hydrological year 2022/2023 give an estimated mass change of –196 Gt for Greenland, close to the long-term rate of mass loss from the ice sheet. The Antarctic ice sheet gained 122 Gt over this same period.

GLACIERS

Preliminary data indicate the annual mass balance of a global set of reference glaciers for the hydrological year 2022/2023 was –1.2 m of water equivalent. This is nominally the largest loss of ice on record (1950–2023), driven by extremely negative mass balance in both western North America and Europe.

Glaciers in western North America and the European Alps experienced an extreme melt season. In Switzerland, glaciers have lost about 10% of their remaining volume in the past two years.

Glaciers are formed from snow that has compacted to form ice, which then deforms and flows downhill. Glaciers comprise two zones: an accumulation zone, where accumulation of mass from snowfall exceeds ice loss, and an ablation zone, where ice loss (ablation) from melting and other mechanisms exceeds accumulation. Where glaciers end in a lake or the ocean, ice loss can occur through melting where the ice meets the water, and via calving, when chunks of the glacier break off.

Glacier mass balance – the amount of mass gained or lost by the glacier – is commonly expressed as the annual thickness change averaged over the glacier area, in turn expressed in metres of water equivalent (m w.e.).[51] Melt rates are strongly affected by glacier albedo, the fraction of sunlight that is reflected by the glacier surface. Exposed glacier ice is darker and therefore has a lower albedo than the seasonal snowpack; it is also sensitive to darkening from mineral dust, black carbon, algal activity and fallout from forest fires. Reduced snow cover, long melt seasons and wildfire activity all serve to concentrate darker material on the glacier surface, decreasing its albedo and thereby increasing melt.

Preliminary data from a set of reference glaciers monitored by the World Glacier Monitoring Service (WGMS) indicate a global annual mass balance for the hydrological year 2022/2023 of –1.2 m w.e., which is slightly more negative than 2021/2022 for the set of about 60 WGMS reference glaciers. Based on the available glacier data, this is nominally a record low mass balance (1950–2023, see Figure 16). Record loss was driven by extremely negative mass balance in both western North America and Europe, and 7 out of the 10 most negative mass-balance years have occurred since 2010.

The annual mass loss for Swiss glaciers in 2022–2023 was the second largest on record (from 1950 to present, see Figure 17) at 4.4% of the remaining ice volume. Together with the record mass loss in 2021–2022 of 5.9%, Swiss glaciers have lost about 10% of their remaining volume in just two years. This has been driven by low snowpacks and warm summers each year, with potential cumulative impacts from glacier darkening associated with longer-than-normal periods of exposed glacier ice and loss of high-elevation firn.[53]

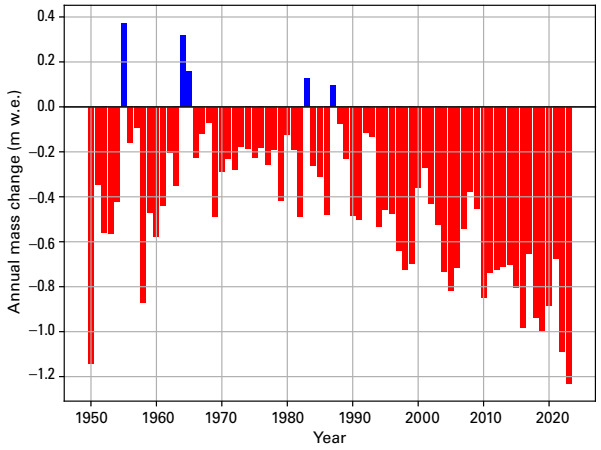

Figure 16. Annual mass balance of reference glaciers with more than 30 years of ongoing glaciological measurements. Annual mass change values are given on the y-axis in the unit meter water equivalent (m w.e.) which corresponds to tonnes per square meter (1 000 kg·m^{-2}).

Source: WGMS (2023, updated and earlier reports[52])

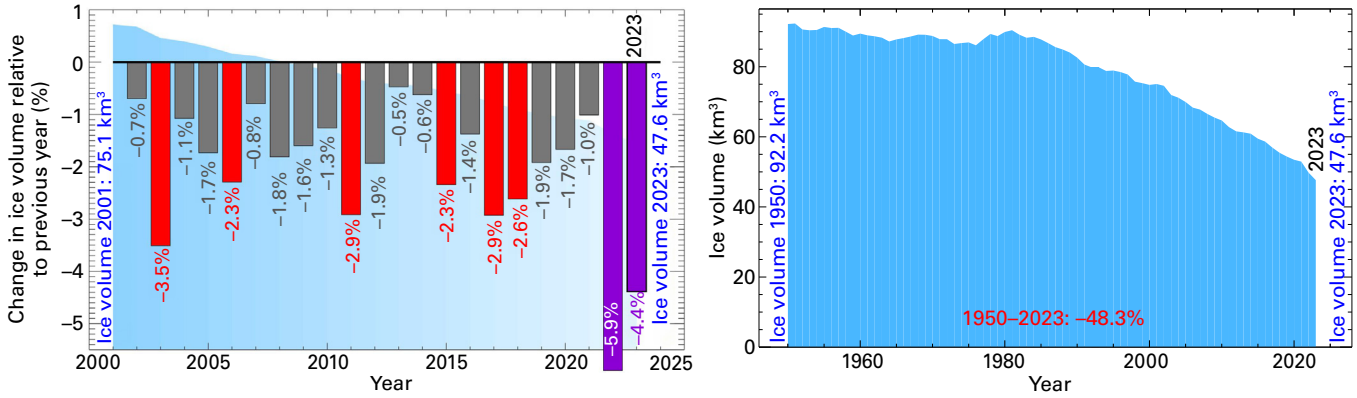

Figure 17. (left) Total annual loss of Swiss glaciers related to current ice volume. The vertical bars indicate the percentage change in ice volume relative to the previous year. Red and purple bars are the eight largest relative mass losses on record. The purple bars are the relative mass losses for 2022 and 2023. The blue shaded area in the background represents overall ice volume as also shown in the right-hand graph. (right) Overall ice volume for Swiss glaciers 1950–2023.

Source: Matthias Huss, based on Glacier Monitoring Switzerland, 2022: *Swiss Glacier Mass Balance (Release 2023)*, https://doi.org/10.18750/massbalance.2022.r2022.

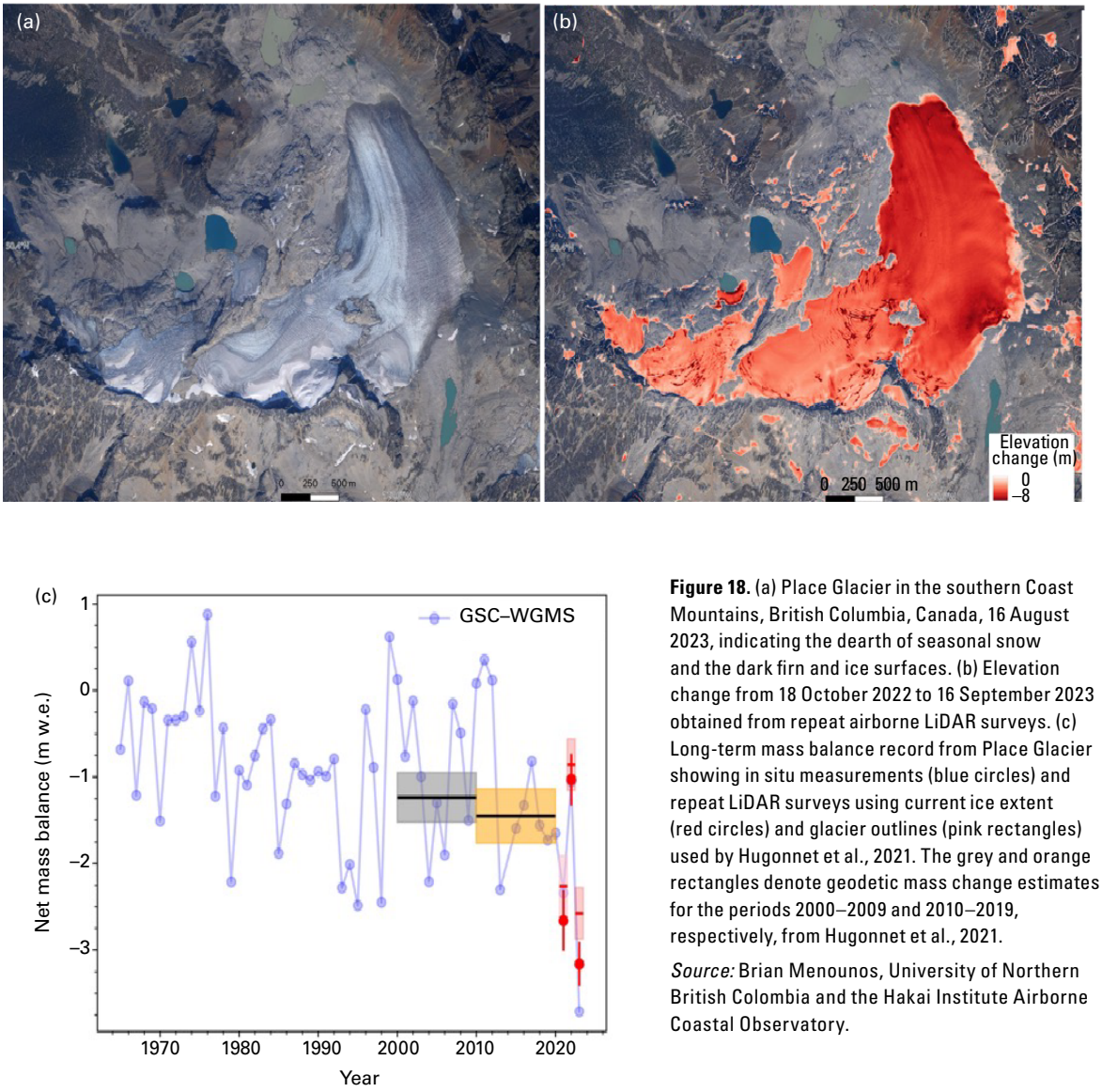

Figure 18. (a) Place Glacier in the southern Coast Mountains, British Columbia, Canada, 16 August 2023, indicating the dearth of seasonal snow and the dark firn and ice surfaces. (b) Elevation change from 18 October 2022 to 16 September 2023 obtained from repeat airborne LiDAR surveys. (c) Long-term mass balance record from Place Glacier showing in situ measurements (blue circles) and repeat LiDAR surveys using current ice extent (red circles) and glacier outlines (pink rectangles) used by Hugonnet et al., 2021. The grey and orange rectangles denote geodetic mass change estimates for the periods 2000–2009 and 2010–2019, respectively, from Hugonnet et al., 2021.

Source: Brian Menounos, University of Northern British Colombia and the Hakai Institute Airborne Coastal Observatory.

Western North America experienced record (from 1965 to present) glacier mass loss in 2023, with glacier-averaged annual thinning of more than 3.5 m at LiDAR-monitored[54] glacier sites in the Canadian Rockies and southern Coast Mountains. Based on regional LiDAR surveys, North American glaciers lost mass at rates that were five times higher than rates measured for the period 2000–2019.[55] Adjusting the LiDAR altimetry data for snow and ice density, estimates of mass balance at two sites with long-term measurements, Place (see Figure 18) and Haig Glaciers, are, respectively, 3.1 ± 0.5 m w.e. and –3.8 ± 0.6 m w.e. In situ mass balance measurements from these two sites give estimates of –3.7 m w.e. and –4.1 m w.e., respectively; far below the long-term mean and more than 1 m w.e. below the previous record minima.

The large negative mass balances are due to a below-average winter snowpack followed by an intense spring heatwave that led to early exposure of bare ice across most glaciers and icefields in south-west Canada. Seasonal snow was mostly gone in midsummer on most glaciers, exposing darker firn or ice over an extended melt season (see Figure 17). Above-average summer temperatures and record wildfire activity in western Canada[56] (see Extreme weather and climate events) contributed to the extreme melt, with particulate deposition

from the wildfires further darkening the glacier surfaces. High rates of cumulative melting over the past several years may also be a factor, as impurities are increasingly concentrated on the glacier surfaces and the firn zone has been lost on many mountain glaciers. These factors are becoming persistent, and glaciers in western North America lost an estimated 9% of their 2020 volume over the period 2020–2023.

SNOW COVER

Seasonal snow cover in the northern hemisphere has been experiencing a long-term decline in the late spring and summer. Northern hemisphere snow-cover extent for May was the eighth lowest on record (1967–2023). North American snow-cover extent for May 2023 was the lowest on record (1967–2023).

Seasonal snow cover in the northern hemisphere has been experiencing a long-term decline in the late spring and summer, which continued in 2023. Northern hemisphere snow-cover extent from January through April 2023 was close to the long-term average (1991–2020), but the spring heatwave in North-western North America drove widespread snowmelt. North American snow-cover extent for May 2023 was the lowest on record (1967–2023) at 7.47 million km^2, about 1.57 million km^2 (17%) below the long-term average, while overall northern hemisphere snow-cover extent was 16.74 million km^2, the eighth lowest since 1967 and 1.47 million km^2 below the long-term average (see Figure 19).

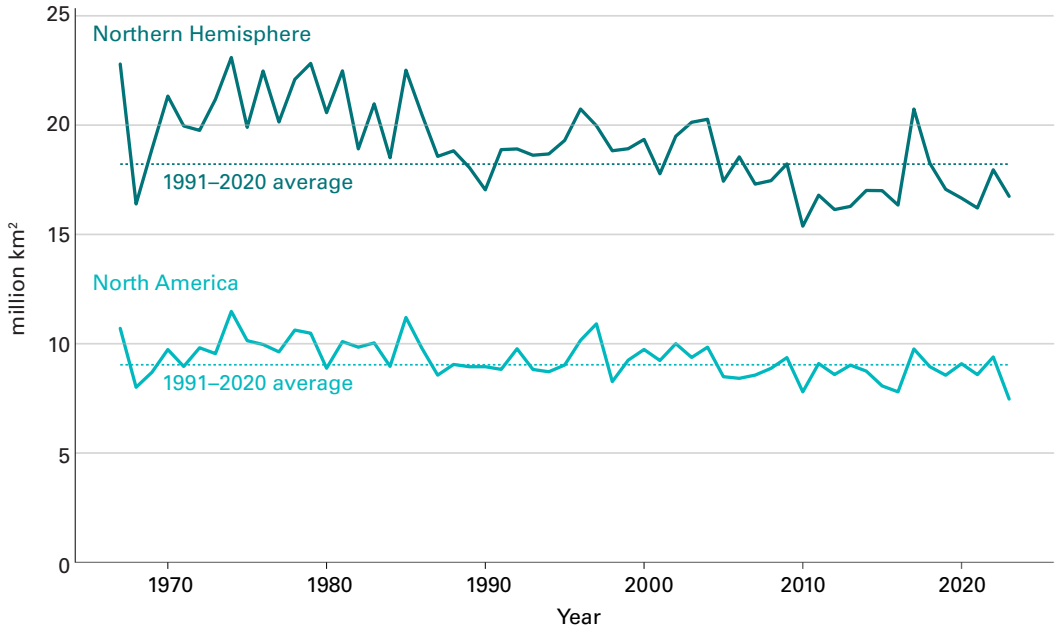

Figure 19. May snow-cover extent for the northern hemisphere (dark blue) and North America (light blue), 1967–2023. The 1991–2020 average for each region is shown as a horizontal dotted line.

Source: Data from the Rutgers University Global Snow Lab[57].

Climate Monitoring and Renewable Energy

Hamid Bastani and Roberta Boscolo

Renewable energy generation, primarily driven by the dynamic forces of solar radiation, wind and the water cycle, has surged to the forefront of climate action for its potential to achieve decarbonization targets. Worldwide, a substantial energy transition is already under way. In 2023, renewable capacity additions increased by almost 50% compared with 2022, for a total of 510 GW.[58] Such growth marks the highest rate observed in the past two decades and, as the International Energy Agency (IEA) indicates, demonstrates the potential to achieve the clean energy goal set at the twenty-eighth United Nations Climate Change Conference (COP 28) to triple renewable energy capacity globally to reach 11 000 GW by 2030.[59]

In the era of this massive and fast transition to renewables, understanding the critical nexus between climate variability and renewable energy is pivotal. A comprehensive knowledge of how the climate is going to modulate the availability of and demand for renewable energy is essential for optimizing the operation and planning of, and investments in, energy resources. The recent joint publication of WMO and the International Renewable Energy Agency (IRENA), *2022 Year in Review: Climate driven Global Renewable Energy Potential Resources and Energy Demand*, underscores the inherent links between renewable energy resources and weather and climate conditions. The publication emphasizes the potential for developing countries – especially in Africa, where energy access remains a key priority – to develop clean energy systems and urges better accounting for climate variability for the improved operation, management and planning of energy resources.

The importance of accounting for climate variability can be seen in Figure 21, which shows monthly energy supply and demand anomalies in Botswana, Mozambique, Namibia, South Africa and Zimbabwe in 2022 relative to the average of the 1991–2020 reference period. The anomalies are measured by four defined energy indicators, which are capacity factors[60] for wind power, solar photovoltaic power, weighted total precipitation as a proxy indicator for hydropower and energy degree days as a proxy indicator for energy demand.

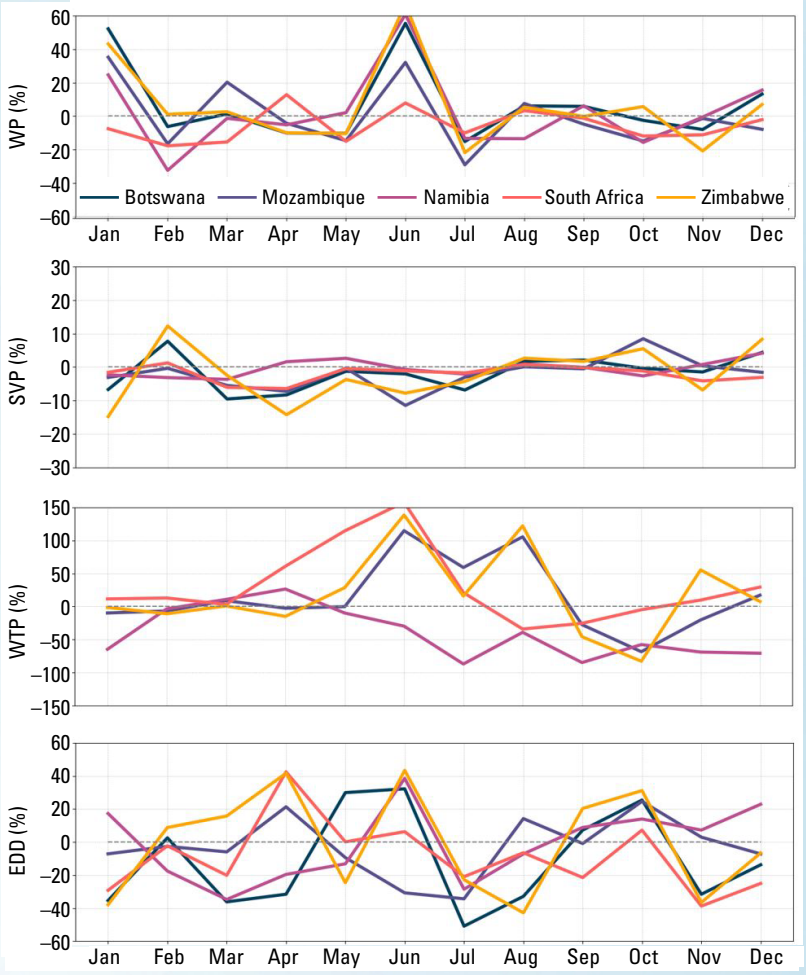

To illustrate how the plots can be interpreted, consider October, when demand in all five countries is between 5% and 30% higher than average, while a large portion of potential generation is lower than average (except for small increases in solar photovoltaic power in Mozambique and Zimbabwe, and wind power in Zimbabwe). In this situation, balancing power would require careful planning, for instance to ensure there were enough water in hydropower dams from the previous rainy season (typically ending in May) ahead of the next rainy season (typically starting in October–November).

For more detailed information about the indicators and additional insights as to other regions and global results, refer to the publication.[61]

Figure 20. Monthly percentage anomalies of four energy indicators for wind power (WP), solar photovoltaic (SPV) power, weighted total precipitation (WTP) (hydropower proxy indicator) and energy degree days (EDD) (energy demand proxy indicator) for 2022 relative to corresponding months in the 1991–2020 reference period for five countries in southern Africa as indicated in the legend. Note that Botswana does not have hydropower plants, and therefore no indicator has been computed. Also note that the y-axis varies depending on the range of the indicator.

Source: WMO–IRENA

STRATOSPHERIC OZONE AND OZONE-DEPLETING GASES

Following the success of the Montreal Protocol, the use of halons and chlorofluorocarbons (CFCs) has been reported as discontinued, but their levels in the atmosphere continue to be monitored.[62] Owing to the long lifetimes of CFCs, these compounds will remain in the atmosphere for many decades and, even if there were no new emissions, there would still be more than enough chlorine and bromine present to cause the complete destruction of the ozone in Antarctica from August to December. As a result, the formation of the Antarctic ozone hole continues to be an annual spring event, with year-to-year variation in its size and depth governed to a large degree by meteorological conditions. The "hole" is not, strictly speaking, a hole; it is an area where the total column ozone in the stratosphere falls below 220 Dobson units.[63]

In 2023, the development of the ozone hole had an unusually early start, becoming the sixth largest in the satellite era. It expanded to 26 million km2 on 21 September (see Figure 20), comparable with the two previous years (2021 and 2022) and close to the maxima observed in earlier years, such as 28.2 million km2 in 2015 and 29.6 million km2 in 2006, according to analyses from the National Aeronautics and Space Administration (NASA)[64] and the Copernicus Atmosphere Monitoring Service (CAMS)[65]. NASA reported a minimum ozone of 99 Dobson units on 3 October 2023. Despite the area of the ozone hole decreasing in a typical manner through early October, it increased again towards the end of the month and remained at or above approximately 15 million km^2 until the first week of December. Although the ozone hole was unusually long-lived in 2023, its longevity was similar to that of the ozone holes of the past three years.

The unusual persistence of the ozone holes of the past three years was due to below-average stratospheric temperatures and a strong polar vortex lasting until December. Several potential drivers for the observed stronger polar vortex have been identified, including water vapour injected into the stratosphere by the eruption of Hunga Tonga–Hunga Ha'apai, wind patterns in the southern hemisphere and climate change.

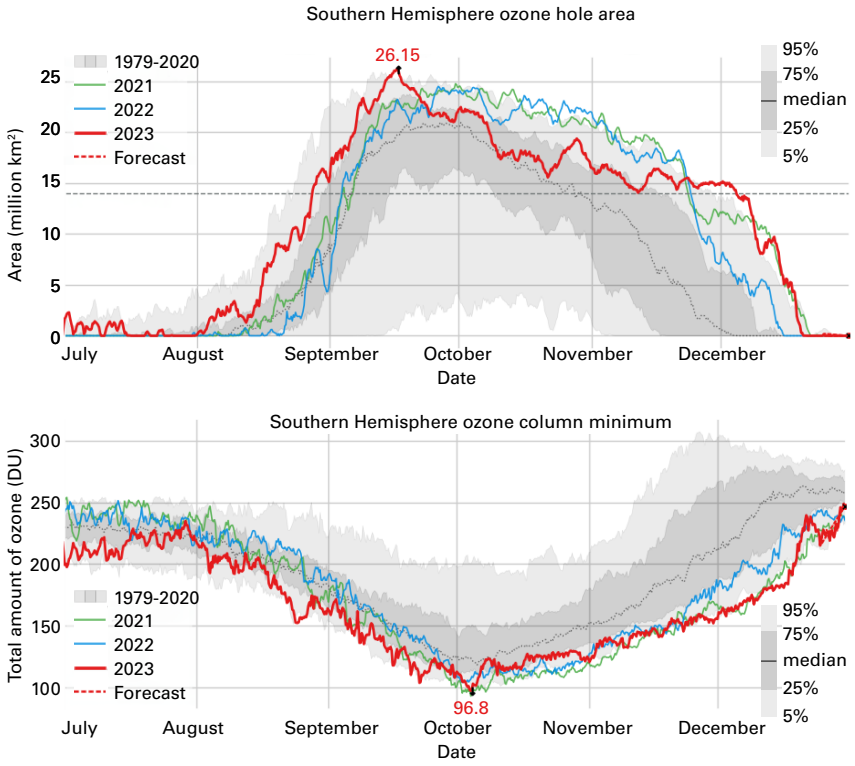

Figure 21. Area (millions of km2) and minimum ozone where the total ozone column is less than 220 Dobson units; 2023 is shown in red. The three most recent years are shown for comparison, as indicated by the legend. The smooth, thick grey line is the 1979–2020 average.

Source: Copernicus Atmosphere Monitoring Service (CAMS)

SHORT-TERM CLIMATE DRIVERS

A prolonged period of La Niña from mid-2020 to early 2023 gave way to El Niño conditions, which were well established by September 2023, contributing to the observed rise in global mean sea-surface temperatures during 2023.

There are many different natural phenomena, often referred to as climate patterns or climate modes, that affect weather and climate at timescales ranging from days to several months or even years. In 2023, the El Niño–Southern Oscillation (ENSO), the Indian Ocean Dipole (IOD) and the North Atlantic Oscillation (NAO), highlighted here, contributed to major weather and climate events across large areas of the world.

ENSO – EL NIÑO SOUTHERN OSCILLATION

ENSO is one of the most important climate drivers of year-to-year variability in weather patterns worldwide. It is linked to hazards such as heavy rains, floods, droughts, heatwaves and cold spells. El Niño, characterized by higher-than-average sea-surface temperatures (SSTs) in the eastern tropical Pacific and a weakening of the trade winds, typically has a warming influence on global temperatures. La Niña, which is characterized by below-average SSTs in the central and eastern tropical Pacific and a strengthening of the trade winds, has the opposite effect.

A multi-year La Niña event began in mid-2020 and ended in early 2023. Subsequently, SSTs in the eastern tropical Pacific increased, crossing typical El Niño thresholds (0.5 °C in Figure 22 (see below)) by June. However, the atmosphere was slower to respond, and it was not until early September that El Niño conditions were well established in both the atmosphere and ocean. By the end of the year, a strong El Niño had developed, with the Oceanic Niño Index reaching 2.0 °C for the November–January period, the highest value since the 2015/2016 El Niño.

El Niño has an influence on regional rainfall patterns. Precipitation anomalies were typical of El Niño in some regions, including drier-than-usual conditions in maritime South-East Asia and from southern Mexico to northern South America, and wetter-than-normal conditions in parts of Chile (see Figure 23 below).

Decreased monsoon rainfall in South-East Asia is associated with El Niño. The onset of the monsoon over Kerala, India, occurred on 8 June, seven days later than normal. By the end of September, India had received 94% of its typical monsoon rainfall.[66] Higher-than-normal rainfall totals, however, were observed along the lower course of the Indus River and in central India.

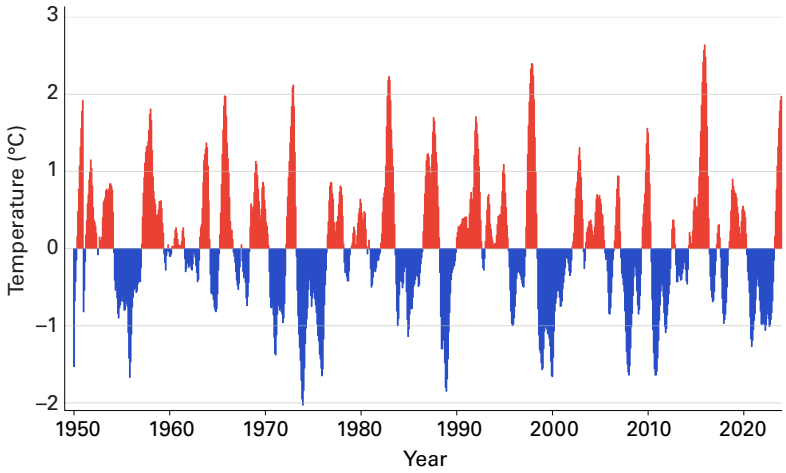

Figure 22. Time series of NOAA's Oceanic Niño index from January 1950 to December 2023 showing the presence of cooler-then-average conditions (blue) and warmer-than-average conditions (red) during 3-month average time periods. Anomalies are with respect to the 1991–2020 average sea-surface temperature.

Source: NOAA NCEP

In Australia, La Niña is associated with wetter-than-normal conditions, and El Niño with drier-than-normal conditions. In January, rainfall for the country was 35% above normal as La Niña drew gradually towards an end, but in August it was 50% below normal with a strengthening El Niño. The dryness was also accompanied by the highest July-to-September national mean temperatures in the country's 114-year record. September was the driest on record in Australia, and August–October was the driest three-month period in the 124-year observational record. However, somewhat atypically for an El Niño event, November and December were wetter than average in much of eastern Australia.

As average global temperature anomalies increased during the transition from La Niña to El Niño, many regions also experienced heatwaves, including parts of China, Europe, Mexico, North Africa and the Middle East, Siberia, South America and the United States of America. A United Nations Environment Programme (UNEP) Frontiers report[67] hhighlighted that variability associated with El Niño has implications for biomass and fire weather,[68] which increases the risk of large and intense wildfires in some places. Please refer to Extreme weather and climate events for more details on extreme events.

INDIAN OCEAN DIPOLE

The positive phase of the IOD is characterized by below-average SSTs (and sea level) in the eastern Indian Ocean and above-average SSTs (and sea level) in the west. The negative phase has the opposite pattern. The resulting change in the gradient of SST across the ocean basin affects the weather of the surrounding continents, primarily in equatorial regions and the southern hemisphere. Positive IOD events are often, but not always, associated with El Niño, and negative events with La Niña.

In conjunction with the emergence of El Niño, the first positive IOD since 2019 developed in early austral spring and peaked during October 2023. The positive IOD helped to intensify the anomalously dry and warm conditions over parts of Australia during this time. Conversely, rainfall totals in the Horn of Africa during the October–December rainy season were much higher than normal, leading to flooding in Ethiopia, Kenya and Somalia; this follows the prolonged drought in the region from 2020 to early 2023, when La Niña conditions and a neutral to negative IOD were largely present.

NORTH ATLANTIC OSCILLATION

Average sea-level pressure in the North Atlantic is characterized by an area of lower pressure close to Iceland, known as the Icelandic low, and an area of higher pressure centred over the Azores, known as the Azores high. The NAO is based on the sea-level pressure difference between the Icelandic low and the Azores high. It is mainly associated with driving weather conditions in the North Atlantic basin, Europe and the Mediterranean. The positive phase is characterized by below-normal pressure over the North Atlantic and high latitudes, and above-normal pressure over the central Atlantic, the eastern United States and western Europe. The negative phase has the opposite pattern. As the phases are determined by pressure changes in the atmosphere, they can fluctuate more rapidly, from days to weeks, compared with other climate drivers such as ENSO, which are driven by slower changes in ocean temperature and fluctuate from months to years.

High pressure associated with the negative NAO in late June and July 2023 contributed to a heatwave that caused significant snowmelt and ice melt across southern Greenland. Several widespread melting events occurred during this period. Ireland reported its warmest June on record (124 years), as did the long-running Uccle station in Belgium (191 years). In eastern Canada, many locations reported record warmth for July.

PRECIPITATION

Accumulated precipitation totals in 2023 were above the long-term average (see Figure 23) in East and Central Asia and parts of northern Asia; the western Indian summer monsoon region; parts of the Maritime Continent; northern New Zealand; parts of West, Central, southern and East Africa; western, Central and South-East Europe; southern Scandinavia; the western Middle East; North-West, South-West and South-East North America; the Greater Antilles; and parts of South-East South America.

Regions with a marked rainfall deficit included South-East South America, the Amazon basin and much of Central America; southern Canada; the western Mediterranean region and South-West Europe; parts of North-West, Central and southern Africa; parts of Central Asia; the eastern Indian monsoon region; parts of South-East Asia and the Maritime Continent; south-west and coastal north Australia; and many of the Pacific Islands.

The onset of the West African monsoon was around normal. The Greater Horn of Africa region, which had been experiencing long-term drought, suffered substantial flooding in 2023, particularly later in the year as heavy rains associated with El Niño and the positive IOD became established (see Extreme weather and climate events).

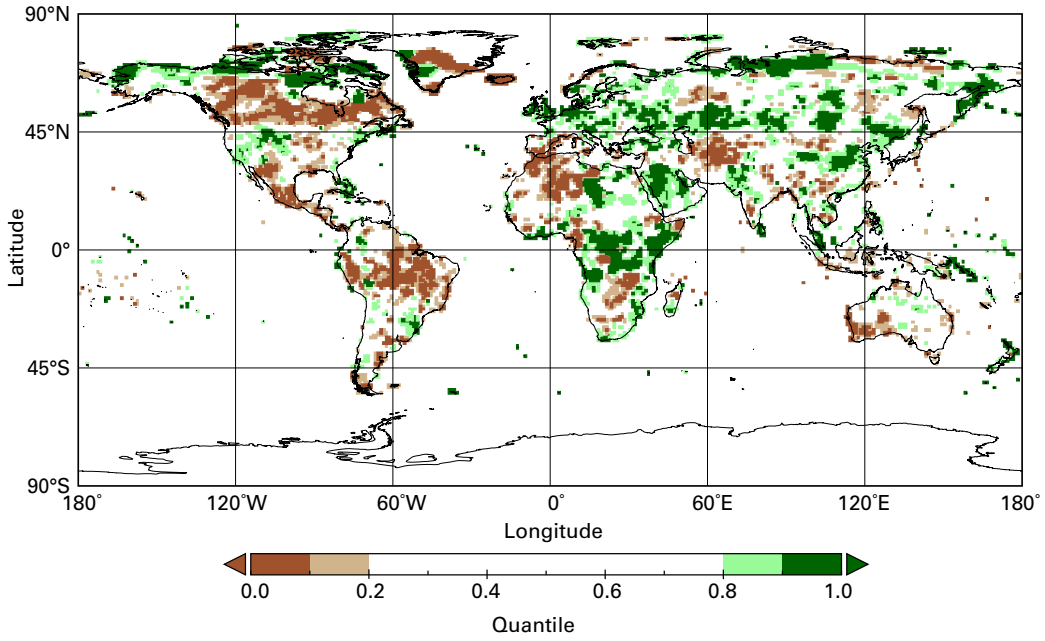

Figure 23. TTotal precipitation in 2023, expressed as a quantile of the 1991–2020 reference period, for areas that would have been in the driest 20% (brown) and wettest 20% (green) of years during the reference period, with darker shades of brown and green indicating the driest and wettest 10%, respectively.

Source: Global Precipitation Climatology Centre (GPCC), Deutscher Wetterdienst (DWD), Germany. For more details, see Data set and methods

Extreme weather and climate events

Extreme weather continues to lead to severe socioeconomic impacts.

Extreme heat affected many parts of the world.

Wildfires in Canada, Europe and Hawaii (United States of America) led to loss of life, the destruction of homes and large-scale air pollution.

Flooding associated with extreme rainfall from Mediterranean Cyclone *Daniel* affected Greece, Bulgaria, Türkiye and Libya, with particularly heavy loss of life in Libyaa.

Extreme weather and climate events had major impacts on all inhabited continents in 2023. These included major floods (some of them associated with tropical cyclones), extreme heat and droughts, and associated wildfires, which presented challenges to water and food security as well as to human welfare.[69,70] Some of the most significant events are described below, with a broader range of events described in the online supplement.

One of the most significant single weather-related events in terms of loss of life was the Mediterranean cyclone (or "medicane"), referred to locally as Storm *Daniel*, in September. In its initial stages, the storm produced extreme rainfall in southern Bulgaria, Greece and parts of Türkiye, while at the same time another storm system produced significant flash flooding in Spain, with adverse effects on cereal production.[71] The heaviest falls were in the Thessaly region of Greece, to the north of Athens, where Zagora, Pelion, received 760 mm on 5 September and a five-day total of 1 096 mm from 4 to 8 September, while in Bulgaria 329 mm fell in 16 hours at Kosti on 4–5 September. The storm then remained slow-moving in the eastern Mediterranean for several days before its major rainbands impacted north-eastern Libya on 10 and 11 September. Extreme rainfalls affected the coast and nearby mountains, with 414 mm falling in 24 hours at Al-Bayda on 10–11 September. The intense rainfalls resulted in extreme flooding in the region. The most extreme impacts were in the city of Derna (about 50 km east of Al-Bayda), where much of the central city was destroyed by flooding that was exacerbated by the failure of two dams. At least 4 700 confirmed deaths in Libya have been attributed to the flooding,[72] with 8 000 people still missing (as at 15 December). There were 19 additional deaths in Bulgaria and Greece.[73]

Tropical Cyclone *Freddy* in February and March was one of the world's longest-lived tropical cyclones. It formed on 6 February off the western coast of Australia and, after earlier landfalls in Madagascar and Mozambique, made its final landfall in Mozambique on 11 March before moving inland as a remnant low. The major impacts of *Freddy* came because of flooding during the final landfall, both in Malawi and Mozambique, as extremely heavy rain fell (up to 672 mm during the storm in Mozambique). Parts of Malawi and Mozambique had not yet recovered from storms in 2022. Malawi was especially hard hit, with at least 679 deaths reported and over 659 000 internal displacements,[74] and there were a further 165 deaths in Mozambique.[75] Casualties were also reported in Madagascar and Zimbabwe, and at sea near Mauritius.

Tropical Cyclone *Mocha*, in May, was one of the most intense cyclones ever observed in the Bay of Bengal, reaching peak 10-minute sustained winds of 115 kt. It formed on 11 May and made landfall near the Bangladesh–Myanmar border on 14 May. Cyclone Mocha triggered 1.7 million displacements across the subregion, from Sri Lanka to Myanmar and through India and Bangladesh.[76] In Bangladesh, displacement was reported in Cox's Bazar, the world's largest refugee settlement, which is home to over 900 000 Rohingya refugees from Myanmar.[77] More than 29 000 people were temporarily relocated.[78] In total, at least 156 lives were lost in Myanmar,[79] and over 270 000 buildings were damaged or destroyed.[80] At least 63 000 displacements took place in camps sheltering people already displaced by conflict and violence.[81] The effects of Cyclone *Mocha*, together with an intensification of conflict and record-high food prices, severely aggravated acute food insecurity, especially among the 3.4 million vulnerable people assessed as in need of humanitarian assistance.[82]

The largest reported economic loss from a single event in 2023 was from Hurricane Otis, which hit the Pacific coast of Mexico in late October. Otis reached hurricane intensity at 1200 Universal Time Coordinated (UTC) on 24 October, and within 15 hours had intensified to a category 5 system,[83] one of the most rapid rates of intensification observed in the satellite era. Shortly afterwards, it made landfall just west of Acapulco at near peak intensity, with maximum sustained winds of 260 km hr^{-1}, which might be the first known category 5 landfall on the Pacific coast of Mexico. The hurricane caused widespread destruction in Acapulco and surrounding areas, with economic losses estimated at 12 billion US dollars (USD).[84] At least 48 deaths were attributed to the hurricane,[85] with a further 32 people missing, mostly at sea.

The North Island of New Zealand suffered repeated extreme rainfall and flooding events in January and February. The most significant was on 13–14 February, when Cyclone *Gabrielle* passed just east of North Island as a post-tropical system. Daily rainfalls exceeded 500 mm in parts of eastern North Island, and Auckland had its lowest air pressure (971.5 hPa) on record. Eleven deaths were reported because of *Gabrielle*, and four by more localized floods in Auckland on 27–28 January. Total economic losses from the two events were estimated at USD 5.3–USD 8.6 billion,86 by far the costliest non-earthquake disaster recorded in New Zealand.

Many significant heatwaves occurred in various parts of the world during 2023. Some of the most significant were in southern Europe and North Africa, especially in the second half of July, when severe and exceptionally persistent heat occurred. Italy was particularly affected, with temperatures reaching 48.2 °C on 24 July at Lotzorai and Jerzu, Sardinia; only 0.6 °C below the European record set in Sicily in 2021.[87] On 23 August, a mean daily temperature of 32.98 °C was reported at the Brera Observatory in Milan, the highest in a record dating back to 1763. Among the other locations experiencing record-high temperatures were Tunis (49.0 °C on 24 July), Tirana (43.0 °C on 25 July), Agadir (Morocco) (50.4 °C on 11 August) and Algiers (49.2 °C on 23 July). The extreme heat shifted to South-East Europe in late July, and further heatwaves affected West-Central Europe in late August and early September. Numerous locations in southern France, northern Spain and western Switzerland set records during these events, including Toulouse (France) (42.4 °C on 23 August[88]). There was also extensive wildfire activity during the summer, particularly in Greece (both on the mainland and islands). A fire in north-eastern Greece in late August and early September that burned 96 000 ha was the largest fire ever observed in the European Union.[89]

The 2023 wildfire season in Canada was well beyond any previously recorded. Significant fire activity began in late April, expanded during a very warm, dry May, and continued throughout the summer and into early autumn. The total area burned nationally for the year was 14.9 million ha, more than seven times the long-term average (1986–2022) and far above the previous record seasonal total of 6.7 million ha in 1989 (see Figure 24). Altogether 297 evacuation orders were issued for over 235 000 people.[90] The fires also resulted in significant and widespread smoke pollution, particularly in the heavily populated areas of eastern Canada and the north-eastern United States of America in the first half of June. Four deaths were directly attributed to fires, although the broader health impacts of the smoke are yet to be fully assessed.

The deadliest single wildfire of the year occurred in Hawaii (United States), on the western side of the island of Maui. Extreme fire weather conditions, with low humidity and strong, gusty winds driven by a pressure gradient between strong high pressure to the North and the circulation of Hurricane *Dora* well to the South, combined with pre-existing drought to favour the development and rapid spread of intense fires. The most affected region was around the town of Lahaina, which was largely destroyed with over 2 200 structures lost. Mandatory

evacuation notices were issued for 7 500 people across the area.[91] At least 100 deaths were reported,[92] the most in a wildfire in the United States for more than 100 years, with 400 homes destroyed[93] and estimated economic losses of USD 5.6 billion. Wildfires of such intensity and speed of movement are extremely rare in the tropics.

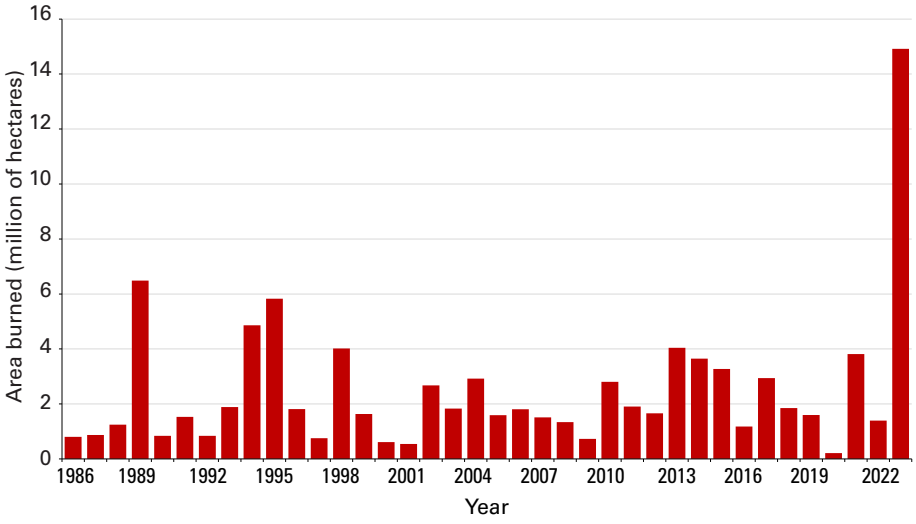

Figure 24. Figure 24. Annual area burned in Canada 1986–2023 (millions of ha)

Source: Data from Jain et al., 2024[94]

Long-term drought persisted in North-western Africa and parts of the Iberian Peninsula, as well as in parts of Central and South-West Asia, and intensified in many parts of Central America, northern South America and the southern United States. Among the most significant areas of drought was an area of subtropical South America, focused on northern Argentina and Uruguay. Rainfall from January to August was 20%–50% below average over much of northern and central Argentina, with some regions experiencing their fourth successive year of significantly below-average rainfall. In Uruguay, water storages reached critically low levels, badly affecting the quality of supplies to major centres, including Montevideo, although there was some improvement in the situation from August. Although there was some easing of drought conditions in subtropical South America later in the year, they intensified in many parts of the continent's interior, including in large parts of the Amazon basin. Eight Brazilian states recorded their lowest July–September rainfall in over 40 years. The Rio Negro at Manaus reached a record low level (observations started in 1902) on 26 October, 0.93 m below the previous record set in 2010.[95]

The Greater Horn of Africa region, which had been experiencing long-term drought, suffered substantial flooding in 2023, particularly later in the year following heavy rains associated with El Niño and the positive Indian Ocean Dipole (IOD) (see Short-term climate drivers). The most badly affected area was the region encompassing south-eastern Ethiopia, north-eastern Kenya and the southern half of Somalia. During the Deyr rainy season (October and November), monthly rainfall in this region was widely 100–200 mm and locally exceeded 200 mm, several times the long-term averages. There were at least 352 deaths reported across the three countries.[96] Throughout Burundi, Ethiopia, Kenya, Somalia, South Sudan, Uganda and the United Republic of Tanzania, widespread and severe flooding displaced 1.8 million people,[97] in addition to the 3 million people already displaced internally or across borders by five consecutive seasons of drought[98] in Djibouti, Ethiopia, Kenya and Somalia. The wet conditions did lead to some recovery in pasture and crop conditions after the extended drought. Landslides and flooding in early December also resulted in at least 89 deaths in northern parts of the United Republic of Tanzania.[99] Pastoralist communities continued to be affected by asset losses after two consecutive years of drought, which continued to adversely affect agricultural production and reduced cereal production in 2023 compared with 2022.[100]

Socio-economic impacts

Food security, population displacements and impacts on vulnerable populations continued to be of mounting concern in 2023, with weather and climate hazards exacerbating the situation in many parts of the world.

Extreme weather and climate conditions continued to trigger new, prolonged and secondary displacement in 2023 and increased the vulnerability of many who had already been uprooted by complex multi-causal situations of conflict and violence.

The development and implementation of local disaster risk reduction strategies has increased since the adoption of the Sendai Framework for Disaster Risk Reduction.

One of the essential components for reducing the impact of disasters is to have effective multi-hazard early warning systems.

The events described above, and many others besides, occur in a broader context. Extreme weather and climate events interact with, and in some cases trigger or exacerbate, situations concerning water and food security, population mobility and environmental degradation.[101,102]

FOOD SECURITY

The number of people who are acutely food insecure worldwide has more than doubled, from 149 million people before the coronavirus disease (COVID-19) pandemic to 333 million people in 2023 (in 78 countries monitored by the World Food Programme (WFP)).[103] Although global hunger levels remained unchanged from 2021 to 2022, they are still far above pre-COVID 19 pandemic levels: in 2022, 9.2% of the global population (735.1 million people) were undernourished, compared with 7.9% (612.8 million people) in 2019 (see Figure 25).[104] The current global food and nutrition crisis is the largest in modern human history.[105] Protracted conflicts, economic downturns and high food prices are at the root of high global food insecurity levels. High food prices are exacerbated by the high costs of agricultural inputs, driven by ongoing and widespread conflict around the world, and high global food insecurity levels are aggravated by the effects of climate and weather extremes. In southern Africa, for example, weather extremes, including the passage of Cyclone *Freddy* in February 2023, have affected areas of Madagascar, southern Malawi, Mozambique and Zimbabwe. Flooding associated with the cyclone submerged extensive agricultural areas and inflicted severe damage on crops, which has exacerbated a slow economic recovery.[106]

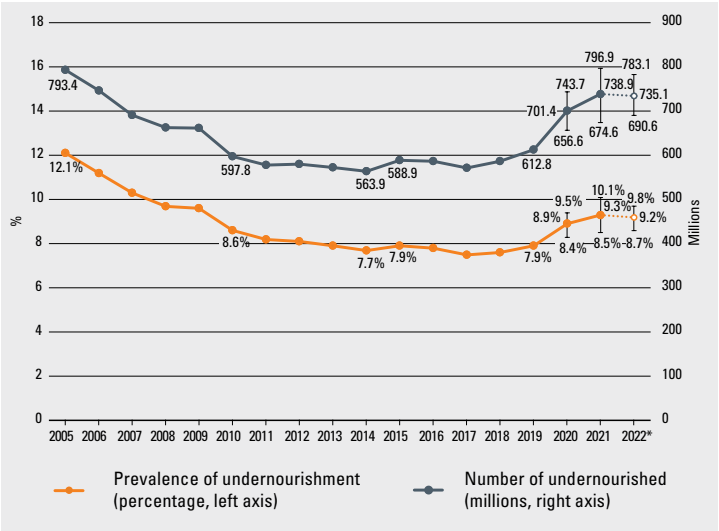

Figure 25. Global prevalence of undernourishment (as a percentage) and number of undernourished (in millions) since 2005

Source: The entire series has been updated to reflect new information released since the publication of *The State of Food Security and Nutrition in the World 2023: Urbanization, Agrifood Systems Transformation and Healthy Diets Across the Rural–Urban Continuum*.[107]

Globally, annual economic losses from climate- and weather-related disasters have increased since the 2000s.[108] Between 2007 and 2022, 88 post-disaster needs assessment surveys conducted in 60 countries worldwide showed that over 65% of losses caused by droughts occur in the agriculture sector, including crop and livestock production losses. For floods, storms and cyclones, about 20% of losses are in agriculture.[109]

In early 2023, South Sudan continued to experience exceptional flooding, with water levels remaining high even during the dry season. Despite relatively dry conditions locally, flooding persisted owing to high flows from further upstream in the Nile basin and very slow drainage from earlier floods. The prolonged flooding made it difficult for people to access basic needs such as food, clean water and health care, and contributed to the near collapse of local livelihoods. Between April and July 2023, 7.8 million people, almost two thirds of the total population of South Sudan, were expected to experience severe acute food insecurity.[110]

Afghanistan experienced a substantial reduction in snowmelt and rainfall, resulting in another poor crop season. This led to widespread acute food insecurity, particularly in the north and north-eastern regions. Between May and October 2023, 15.3 million Afghans were estimated to face severe acute food insecurity.[111] In Yemen, 53% of the population were already classified as in a crisis level of acute food insecurity or worse between October and December 2022. High food and fuel prices, together with floods from March to September 2023, and protracted conflict, further aggravated food insecurity.

In Indonesia, a meteorological drought linked to El Niño and the positive phase of the Indian Ocean Dipole (IOD) (see Short-term climate drivers) occurred during the dry season, affecting 23 450 ha of paddy cultivation and causing 6 964 ha of crop failure as of August 2023. A decrease of 645 000 t of rice production was predicted by October 2023,[112] and crop planting in late 2023 was delayed.

In 2023, record maize production in Brazil compensated for below-average harvests due to prolonged dry spells elsewhere in South America, especially in Argentina, where drought conditions were expected to result in a 15% decrease in cereal production compared with the five-year average. The return of El Niño in 2023 led to adverse consequences through the entire crop cycle of maize in Central America and northern parts of South America, where water deficits and high temperature curtailed both planting area and yields with compounding negative impacts on final production, particularly for smallholders and more vulnerable households in the Dry Corridor. During the second part of the season, tropical storms and unexpected heavy rain events disrupted the normal growth of crops in certain areas near the Central America Pacific coast. In Haiti, irregular seasonal rainfall, including periods of high-intensity precipitation, contributed to decrease the production of primary crops In 2023, record maize production in Brazil compensated for below-average harvests due to prolonged dry spells elsewhere in South America, especially in Argentina, where drought conditions were expected to result in a 15% decrease in cereal production compared with the five-year average. The return of El Niño in 2023 led to adverse consequences through the entire crop cycle of maize in Central America and northern parts of South America, where water deficits and high temperature curtailed both planting area and yields with compounding negative impacts on final production, particularly for smallholders and more vulnerable households in the Dry Corridor. During the second part of the season, tropical storms and unexpected heavy rain events disrupted the normal growth of crops in certain areas near the Central America Pacific coast. In Haiti, irregular seasonal rainfall, including periods of high-intensity precipitation, contributed to decrease the production of primary crops.[113]

Oceania is expected to experience the sharpest annual reduction rate in cereal production worldwide, with a 31.1% decline in 2023 compared with 2022, although this largely reflects a reversion to near-average conditions after exceptionally high production in 2022, with 2023 only slightly below five-year averages.[114]

In September, Storm Daniel brought heavy rainfall to coastal and north-eastern Libya, flooding nearly 3 000 ha of cropland, particularly in the Al Marj and Derna regions. These constitute the main cropland areas in the eastern part of the country and are key sources of livelihoods. The collapse of dams in Derna affected the irrigation system, and the floods affected many parts of the agrifood value chain, damaging roads, cereal storage and overall market channels. According to the Food and Agriculture Organization of the United Nations (FAO) Global Information and Early Warning System (GIEWS), Libya was already in a state of food crisis and in need of external assistance in July 2023 before the floods.[115]

DISPLACEMENT

Across the globe, millions of people, including internally displaced persons, refugees and migrants, are on the move or have been forced to flee their homes and communities because of disasters exacerbated by climate stresses and shocks. Weather hazards continued to trigger new, prolonged and secondary displacement in 2023 and increased the vulnerability of many who had already been uprooted by complex multi-causal situations of conflict and violence. These trends are a clear indication of how vulnerability to climate shocks and stresses is undermining resilience and creating new protection risks, which threatens the achievements of the Sustainable Development Goals (SDGs).

An estimated 3.4 million refugees and internally displaced people in Egypt, Iraq, Jordan, Lebanon and the Syrian Arab Republic were in need of critical assistance to cope with extreme winter conditions in 2023.[116] In the north-west of the Syrian Arab Republic, snowstorms and floods triggered displacements between January and March, many of which were repeated movements of people already displaced by the country's long-running conflict. Similarly, in Yemen, heavy rains hit the country in April. Some sites for internally displaced people in Marib were damaged, leaving dozens of people dead and injured.[117]

Many migrants entering Somalia found themselves stranded in June and July 2023, mostly in the city of Bossaso, the main coastal crossing location to Yemen, as they were waiting for more favourable weather conditions to cross the Gulf of Aden. In Hargeisa, a group of migrants in transit suffered from extreme heat, and some died from dehydration.[118]

In addition to new displacements caused by high-impact disasters in 2023, many people are still enduring the prolonged effects of climate-related displacements that took place in previous years. In Pakistan, the 2022 monsoon floods, which triggered the largest disaster displacement event in a decade, continued to have long-standing impacts in 2023. Displaced communities were still recovering when heavy rains hit some districts in June 2023, causing waterborne and vector-borne diseases.[119]

Displacement in the context of climate change and environmental degradation is often multi-causal. Most people move owing to a combination of social, political, economic, environmental and demographic drivers, all of which are and will continue to be affected by climate and environmental change. In Somalia alone, some 531 000 displacements were recorded related to the ongoing drought in 2023, in addition to 653 000 displacements primarily caused by conflict.[120] Subsequent flooding during the October–December rainy season affected more than 2.4 million individuals, displacing over 1 million people.[121] Estimates for Storm Daniel indicate close to 45 000 individuals displaced in north-eastern Libya.[122] Additionally, a substantial number of migrants were reported to be living in a low-lying area adjacent to Wadi Derna, raising concerns that the floods may have destroyed many of their settlements with significant loss of life.[123]

Climate-related shocks and stresses in migration and displacement contexts affect people's livelihoods, which entrenches poverty (SDG) 1[124] and hunger (SDG 2);[125] pose direct threats to lives and well-being (SDG 3);[126] widen inequality gaps (SDG 10);[127] and limit access to quality education (SDG 4),[128] water and sanitation (SDG 6),[129] as well as to clean energy (SDG 7).[130] Women and girls are among the worst affected (SDG 5)[131] owing to pre-existing gender and socioeconomic inequalities compounding their vulnerabilities.[132]

To better prepare for these contexts, governments, communities, civil society and the United Nations are engaged at all levels to strengthen climate resilience and effective disaster risk reduction. A main priority is the community level, where preparedness efforts, including early warning systems and emergency preparedness, are accelerating.[133] A total of 126 countries are in possession of disaster risk management strategies, with 99 countries reporting to have local governments with disaster risk reduction strategies. The development and implementation of local disaster risk reduction strategies has increased since the adoption of the Sendai Framework for Disaster Risk Reduction in 2015.[134]

One of the essential components for reducing the impact of disasters is to have effective multi-hazard early warning systems (MHEWSs), and systems in place for generating disaster risk information and creating and disseminating early warnings, as well as having plans to act on the warnings. As at 2023, 102 countries reported having MHEWSs in place – more than half the countries in the world. The Early Warnings for All initiative was launched by the Secretary-General of the United Nations in March 2022 with the aim of ensuring that everyone on Earth is protected from hazardous weather, water or climate events through life-saving early warning systems by the end of 2027.

The State of Climate Finance

Climate Policy Initiative

In 2021–2022,[1] **global climate flows reached almost 1.3 trillion US dollars (USD), nearly doubling compared with 2019–2020 levels (see Figure 26).** TThis increase was primarily driven by a significant acceleration in mitigation finance, up by USD 439 billion compared with 2019–2020. The remainder of the observed growth in 2021–2022 stemmed from methodological improvements to, and additional data sources used in, the *Global Landscape of Climate Finance*. Despite this growing momentum in climate finance, tracked flows represented only approximately 1% of global gross domestic product (GDP).

Comparing tracked climate finance flows with estimated climate finance needs exposes a large financing gap. In an average scenario,[2] for a 1.5 °C pathway, annual climate finance investments need to grow by more than six times, reaching almost USD 9 trillion by 2030 and a further USD 10 trillion through 2050.

Despite the large financing gap, the cost of inaction is even higher.[3] Aggregating over the period 2025–2100, the total cost of inaction is estimated at USD 1 266 trillion; that is, the difference in losses under a business-as-usual scenario[4] and those incurred within a 1.5 °C pathway. This figure is, however, likely to be a dramatic underestimate of the true cost of inaction, since it does not capture losses to nature and biodiversity, and those induced by conflict and migration, among others. Indeed, the cost of inaction only promises to rise with insufficient mitigation and inadequate adaptation.

Disaggregating global climate finance flows reveals that growth is neither sufficient nor consistent across sectors and regions. The growth in global climate finance in 2021–2022 largely stemmed from significant increases in clean energy investments in only a handful of geographies; China, Brazil, Europe, India, Japan and the United States of America together received 90% of the increase in funds. Other regions, including many climate-vulnerable countries, and other important sectors – for example, agriculture and industry – are being left behind, receiving disproportionately little finance given their significant mitigation potential. In addition, emerging mitigation technologies, including battery storage and hydrogen, are only beginning to attract private finance and are yet to be scaled up.

---

[1] The Climate Policy Initiative (CPI) reports a biennial average to smooth out fluctuations in (annual) data.

[2] Climate finance needs are estimated as a range, including lower-bound, upper-bound and average needs, based on direct investments in climate-specific physical assets and excluding transition-related unabated fossil fuel finance..

[3] Inaction is defined here as the failure to stay within a 1.5 °C pathway; for further details, see Climate Policy Initiative (CPI), 2024: The Cost of Inaction, https://www.climatepolicyinitiative.org/the-cost-of-inaction/#:~:text=CPI's%20estimate%20of%20USD%201%2C266,%2C%20warming%20scenarios%2C%20and%20timeframes.

[4] A business-as-usual scenario is understood here as equivalent to a 3 °C pathway.

Of particular concern, adaptation finance continues to lag. Though adaptation finance reached an all-time high of USD 63 billion in 2021–2022, the global adaptation financing gap is widening, falling well short of the estimated USD 212 billion per year needed up to 2030 in developing countries alone. Tracked adaptation finance remains dominated by public actors (98%), while tracking challenges continue to impede a clear picture of adaptation action by the private sector. The majority of adaptation finance is directed to the water and wastewater sector, reflecting efforts to build resilience to water stress, while other sectors with wide-ranging adaptation potential – for example, agriculture – continue to receive only minimal finance. Mainstreaming adaptation and resilience into development pathways is imperative, particularly in highly vulnerable developing countries.

Moving forward, all actors must urgently work to scale the quantity and quality of climate finance. Key priorities for ensuring more and better climate finance include transforming the financial system with an emphasis on concessional financing and de-risking; bridging climate and development needs; harnessing synergies to deliver co-benefits for both people and nature; mobilizing domestic capital, with an emphasis on enabling policies and regulatory frameworks; and improving the availability and accessibility of quality, granular data to measure and manage progress.

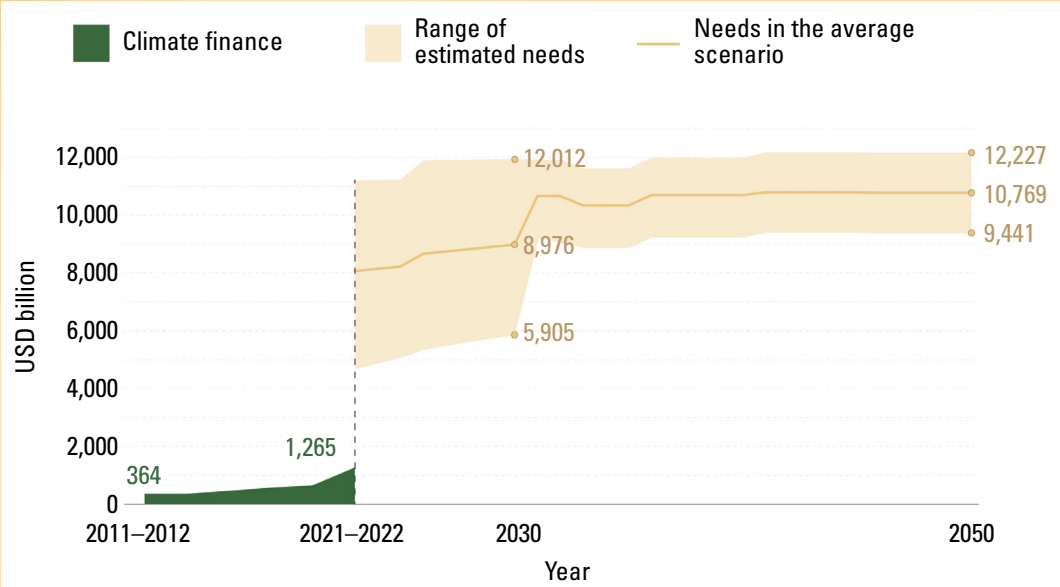

Figure 26. Global tracked climate finance and average estimated annual needs from 2011–2012 through 2050.

Source: Climate Policy Initiative (CPI)

Data sets and methods

GREENHOUSE GASES DATA

Estimated concentrations from 1750 are used to represent pre-industrial conditions. Calculations assume a pre-industrial mole fraction of 278.3 parts per million (ppm) for carbon dioxide (CO_2), 729.2 parts per billion (ppb) for methane (CH_4) and 270.1 ppb for nitrous oxide (N_2O).

World Data Centre for Greenhouse Gases (WDCGG) operated by the Japan Meteorological Agency (JMA), https://gaw.kishou.go.jp.

World Meteorological Organization (WMO). *WMO Greenhouse Gas Bulletin – No. 19: The State of Greenhouse Gases in the Atmosphere Based on Global Observations Through 2022*. Geneva, 2023.

GLOBAL TEMPERATURES DATA

GLOBAL MEAN TEMPERATURE SERIES

The method for calculating global mean temperature anomalies relative to an 1850–1900 baseline is based on the assessment of long-term change and its uncertainty made by Working Group I in its contribution to the Sixth Assessment Report of the Intergovernmental Panel on Climate Change (IPCC AR6 WG I). In 2021, the IPCC AR6 WG I assessed change from 1850–1900 to other periods based on an average of four datasets – HadCRUT5, Berkeley Earth, NOAA Interim, and Kadow et al., 2020 – which start in 1850 and are globally or near-globally complete in the modern period.

To include shorter datasets, which can help to better understand recent temperature changes, in the present publication, the estimate made by the Intergovernmental Panel on Climate Change (IPCC) for the temperature change between 1850–1900 and 1981–2010 is combined with estimated changes between 1981–2010 and the current year from six datasets to calculate anomalies for 2023 relative to 1850–1900. There is good agreement among the datasets on changes from 1981–2010 to the present, as this is a period with good observational coverage.

The additional uncertainty from the spread of the datasets is combined with that of the estimate of the IPCC of the uncertainty in the change from 1850–1900 to 1981–2010. Global mean temperature anomalies were calculated relative to an 1850–1900 baseline using the following steps, starting from the time series of global monthly mean temperatures for each dataset:

1. For each dataset, anomalies were calculated relative to the 1981–2010 average by subtracting the mean for the period 1981–2010 for each month separately.

2. An annual mean anomaly was calculated from the monthly mean anomalies.

3. The amount of 0.69 °C was added to each series, based on the estimated difference between 1850–1900 and 1981–2010, calculated using the method from IPCC AR6 WG I (see the caption for Figure 1.12 in the corresponding publication).

4. The mean and standard deviation of the estimates were calculated.

5. The uncertainty in the IPCC estimate was combined with the standard deviation, assuming the two are independent and assuming the IPCC uncertainty range (0.54 °C–0.79 °C) is representative of a 90% confidence range (1.645 standard deviations).

The number quoted in the present publication for 2023 (1.45 ± 0.12 °C) was calculated in this way, with 1.45 °C being the mean of the seven estimates, and 0.03 °C the standard deviation.

ANNUAL TEMPERATURE MAPS

For the map of temperature anomalies for 2023, a median of six datasets was used, re-gridded to the spatial grid of the lowest resolution datasets (NOAAGlobalTemp and HadCRUT5), which are presented on a 5° latitude by 5° longitude grid. The median is used in preference to the mean to minimize the effect of potential outliers in individual grid cells. The half-range of the datasets provides an indication of the uncertainty. The spread between the datasets is largest at high latitudes and in Central Africa, both regions with sparse data coverage.

GLOBAL MEAN TEMPERATURE ANOMALIES FOR 2023 RELATIVE TO OTHER PERIODS

Table 1 (see below) shows global mean temperature anomalies for individual datasets for 2023 relative to four different baselines. The uncertainty indicated for the three modern baselines (1981–2010, 1991–2020 and 1961–1990) is the standard deviation of the available estimates multiplied by 1.645 to represent the 90% uncertainty range.

Table 1. Global mean temperature anomalies for individual datasets for 2023 for four different baselines

Period	*1850–1900*	*1981–2010*	*1991–2020*	*1961–1990*
HadCRUT5	1.44	0.75	0.56	1.09
NOAAGlobalTemp	1.43	0.74	0.55	1.05
GISTEMP	1.44	0.75	0.56	1.07
Berkeley Earth	1.45	0.76	0.57	1.12
ERA5	1.48	0.79	0.60	1.12
JRA-55	1.43	0.74	0.56	1.07
Mean of the six datasets	1.45±0.12	0.76±0.03	0.57±0.03	1.09±0.04

The following six datasets were used, including four traditional datasets:

Berkeley Earth: Rohde, R.A.; Hausfather, Z. The Berkeley Earth Land/Ocean Temperature Record. *Earth System Science Data* **2020**, *12* (4), 3469–3479. https://doi.org/10.5194/essd-12-3469-2020.

GISTEMP v4: GISTEMP Team, 2022: *GISS Surface Temperature Analysis (GISTEMP), Version 4*. NASA Goddard Institute for Space Studies, https://data.giss.nasa.gov/gistemp/.

HadCRUT.5.0.2.0: Morice, C.P.; Kennedy, J.J.; Rayner, N.A. et al. An Updated Assessment of Near-surface Temperature Change from 1850: The HadCRUT5 Data Set. *Journal of Geophysical Research: Atmospheres* **2021**, *126* (3), e2019JD032361. https://doi.org/10.1029/2019JD032361. HadCRUT.5.0.2.0 data were obtained from http://www.metoffice.gov.uk/hadobs/hadcrut5 on 17 January 2024 and are © British Crown Copyright, Met Office 2024, provided under an Open Government Licence, http://www.nationalarchives.gov.uk/doc/open-government-licence/version/3/.

Lenssen, N.J.L.; Schmidt, G.A.; Hansen, J.E. et al. Improvements in the GISTEMP Uncertainty Model. *Journal of Geophysical Research: Atmospheres* **2019**, *124* (12), 6307–6326. https://doi.org/10.1029/2018JD029522.

NOAAGlobalTemp-Interim v5.1: Vose, R.S.; Huang, B.; Yin, X. et al. Implementing Full Spatial Coverage in NOAA's Global Temperature Analysis. *Geophysical Research Letters* **2021**, *48* (4), e2020GL090873. https://doi.org/10.1029/2020GL090873.

And two reanalyses:

ERA5: Hersbach, H.; Bell, B.; Berrisford, P. et al. *ERA5 Monthly Averaged Data on Single Levels from 1940 to Present*. Copernicus Climate Change Service (C3S) Climate Data Store (CDS), 2023. https://cds.climate.copernicus.eu/cdsapp#!/dataset/10.24381/cds.f17050d7?tab=overview.

JRA-55: Kobayashi, S.; Ota, Y.; Harada, Y. et al. The JRA-55 Reanalysis: General Specifications and Basic Characteristics. *Journal of the Meteorological Society of Japan. Ser. II* **2015**, *93* (1), 5–48. https://doi.org/10.2151/jmsj.2015–001.

IPCC used an additional dataset. Combining the six datasets used in the present publication with Kadow et al., 2020 reduces the estimated global mean for 2023 by 0.01 °C and increases the uncertainty range by a similar amount:

Kadow, C.; Hall, D.M.; Ulbrich, U. Artificial Intelligence Reconstructs Missing Climate Information. *Nature Geoscience* **2020**, *13*, 408–413. https://doi.org/10.1038/s41561-020-0582-5.

A new reanalysis produced by JRA-3Q is now also available. JRA-55 was used in the present publication for consistency with the provisional statement released in December 2023. For comparison, the values for 2023 are shown relative to the four baselines for JRA-3Q and JRA-55 in Table 2 (see below). Note that the replacement of JRA-55 with JRA-3Q in the mean of the six datasets has a negligible effect on the global mean temperature for 2023.

Table 2. Global mean temperatures for 2023 relative to the four baselines for JRA-3Q and JRA-55

Period	*1850–1900*	*1981–2010*	*1991–2020*	*1961–1990*
JRA-3Q	1.47	0.78	0.58	1.11
JRA-55	1.43	0.74	0.56	1.07
Mean of the six datasets using JRA-3Q	1.45±0.12	0.76±0.03	0.57±0.03	1.09±0.04

LAND TEMPERATURES AND SEA-SURFACE TEMPERATURES

The land temperature assessment is based on three data sets:

Berkeley Earth: Rohde, R.A.; Hausfather, Z. The Berkeley Earth Land/Ocean Temperature Record. E*arth System Science Data* **2020**, *12* (4), 3469–3479. https://doi.org/10.5194/essd-12-3469-202.

CRUTEM.5.0.2.0: Osborn, T.J.; Jones, P.D.; Lister, D.H. et al. Land Surface Air Temperature Variations Across the Globe Updated to 2019: The CRUTEM5 Data Set. *Journal of Geophysical Research* **2021**, *126* (2), e2019JD032352. https://doi.org/10.1029/2019JD032352. CRUTEM.5.0.2.0 data were obtained from http://www.metoffice.gov.uk/hadobs/crutem5 on 17 January 2024 and are © British Crown Copyright, Met Office 2024, provided under an Open Government Licence, http://www.nationalarchives.gov.uk/doc/open-government-licence/version/3/.

GHCNv4: Menne, M.J.; Gleason, B.E.; Lawrimore, J. et al. *Global Historical Climatology Network – Monthly Temperature [Global mean]*. NOAA National Centers for Environmental Information, 2017. doi:10.7289/V5XW4GTH.

The sea-surface temperature (SST) assessment is based on two datasets:

HadSST.4.0.1.0: Kennedy, J.J.; Rayner, N.A.; Atkinson, C.P. et al. An Ensemble Data Set of Sea Surface Temperature Change from 1850: The Met Office Hadley Centre HadSST.4.0.0.0 Data Set. *Journal of Geophysical Research: Atmospheres* **2019**, *124* (14), 7719–7763. https://doi.org/10.1029/2018JD029867. HadSST.4.0.1.0 data were obtained from http://www.metoffice.gov.uk/hadobs/hadsst4 on 17 January 2024 and are © British Crown Copyright, Met Office 2024, provided under an Open Government Licence, http://www.nationalarchives.gov.uk/doc/open-government-licence/version/3/.

ERSSTv5: Huang, B.; Thorne, P.W.; Banzon, V.F. et al. *NOAA Extended Reconstructed Sea-Surface Temperature (ERSST), Version 5. [Global mean]*. NOAA National Centers for Environmental Information, 2017. doi:10.7289/V5T72FNM.

OCEAN HEAT CONTENT

The ensemble mean is an update of the outcome of a concerted international effort,[135] and all products used are referenced here. Note that global ocean heat content values are given for the ocean surface area between 60° S and 60° N and limited to areas deeper than 300 m in each product. The value for 2022 is based on a subset of the products for which updates are available. A baseline of 2005–2021 is used for the ocean heat content time series (see Figure 4), as near-global coverage is available for this period thanks to the network of Argo subsurface floats.

The 2023 value is based on the estimate from Minière et al., 2023 and Cheng et al., 2017 (see below):

Minière, A.; von Schuckmann, K.; Sallée, J.-B. et al. Robust Acceleration of Earth System Heating Observed Over the Past Six Decades. *Scientific Reports* **2023**, *13*, 22975. https://doi.org/10.1038/s41598-023-49353-1.

DATA USED UP TO 2022:

Cheng, L.; Trenberth, K.E.; Fasullo, J. et al. Improved Estimates of Ocean Heat Content from 1960 to 2015. *Science Advances* **2017**, *3* (3). https://doi.org/10.1126/sciadv.1601545.

Gaillard, F.; Reynaud, T.; Thierry, V. et al. In Situ–Based Reanalysis of the Global Ocean Temperature and Salinity with ISAS: Variability of the Heat Content and Steric Height. *Journal of Climate* **2016**, *29* (4), 1305–1323. https://doi.org/10.1175/JCLI-D-15-0028.1.

Ishii, M.; Fukuda, Y.; Hirahara, S. et al. Accuracy of Global Upper Ocean Heat Content Estimation Expected from Present Observational Data Sets. *SOLA* **2017**, *13*, 163–167. https://doi.org/10.2151/sola.2017–030.

Kuusela, M.; Giglio, D. *Global Ocean Heat Content Anomalies based on Argo data [2.0.0]*. Zenodo, 2023. https://doi.org/10.5281/zenodo.7562281.

Levitus, S.; Antonov, J.I.; Boyer, T.P. et al. World Ocean Heat Content and Thermosteric Level Change (0–2 000 m), 1955–2010. *Geophysical Research Letters* **2012**, *39* (10). https://doi.org/10.1029/2012GL051106.

Lyman, J.M.; Johnson, G.C. Estimating Global Ocean Heat Content Changes in the Upper 1 800 m since 1950 and the Influence of Climatology Choice. *Journal of Climate*, **2014**, *27* (5), 1945–1957. https://doi.org/10.1175/JCLI-D-12–00752.1.

von Schuckmann, K.; Le Traon, P.-Y. How Well Can We Derive Global Ocean Indicators from Argo Data? *Ocean Science* **2011**, *7* (6), 783–791. https://doi.org/10.5194/os-7-783-2011. Data available at: https://marine.copernicus.eu/access-data/ocean-monitoring-indicators.

IN ADDITION, DATA USED TO 2021:

Desbruyères, D.G.; Purkey, S.G.; McDonagh, E.L. et al. Deep and Abyssal Ocean Warming from 35 Years of Repeat Hydrography. *Geophysical Research Letters* **2016**, *43* (19), 10356–10365. https://doi.org/10.1002/2016GL070413.

Desbruyères, D.; McDonagh, E.L.; King, B.A. et al. Global and Full-depth Ocean Temperature Trends During the Early Twenty-first Century from Argo and Repeat Hydrography. *Journal of Climate* **2017**, 30 (6), 1985–1997. https://doi.org/10.1175/JCLI-D-16-0396.1.

Good, S.A.; Martin, M.J.; Rayner, N.A. EN4: Quality Controlled Ocean Temperature and Salinity Profiles and Monthly Objective Analyses with Uncertainty Estimates. *Journal of Geophysical Research: Oceans* **2013**, *118* (12), 6704–6716. https://doi.org/10.1002/2013JC009067.

Hong, L.; Xu, F.; Zhou, W. et al. Development of a Global Gridded Argo Data Set with Barnes Successive Corrections. *Journal of Geophysical Research: Oceans* **2017**, *122* (2), 866–889. https://doi.org/10.1002/2016JC012285.

Hosoda, S.; Ohira, T.; Nakamura, T. A Monthly Mean Dataset of Global Oceanic Temperature and Salinity Derived from Argo Float Observations. *JAMSTEC Report of Research and Development*, **2008**, *8*, 47–59. https://www.jstage.jst.go.jp/article/jamstecr/8/0/8_0_47/_article.

Kuusela M.; Stein, M.L. Locally Stationary Spatio-temporal Interpolation of Argo Profiling Float Data. *Proceedings of the Royal Society A* **2018**, *474*, 20180400. http://dx.doi.org/10.1098/rspa.2018.0400.

Roemmich, D.; Gilson, J. The 2004–2008 Mean and Annual Cycle of Temperature, Salinity, and Steric Height in the Global Ocean from the Argo Program. *Progress in Oceanography* **2009**, *82* (2), 81–100. https://doi.org/10.1016/j.pocean.2009.03.004.

Roemmich, D.; Church, J.; Gilson, J. et al. Unabated Planetary Warming and its Ocean Structure Since 2006. *Nature Climate Change* **2015**, *5*, 240–245. https://doi.org/10.1038/nclimate2513.

IN ADDITION, DATA USED UP TO 2020:

Church, J.A.; White, N.J.; Konikow, L.F. et al. Revisiting the Earth's Sea-level and Energy Budgets from 1961 to 2008. *Geophysical Research Letters* **2011**, *38* (18). https://doi.org/10.1029/2011GL048794.

Domingues, C.M.; Church, J.A.; White, N.J. et al. Improved Estimates of Upper-ocean Warming and Multi-decadal Sea-level Rise. *Nature* **2008**, *453*, 1090–1093. https://doi.org/10.1038/nature07080.

Li, Y.; Church, J.A.; McDougall, T.J. et al. Sensitivity of Observationally Based Estimates of Ocean Heat Content and Thermal Expansion to Vertical Interpolation Schemes. *Geophysical Research Letters* **2022**, *49* (24), e2022GL101079. https://doi.org/10.1029/2022GL101079.

Wijffels, S.; Roemmich, D.; Monselesan, D. et al. Ocean Temperatures Chronicle the Ongoing Warming of Earth. *Nature Climate Change* **2016**, *6*, 116–118. https://doi.org/10.1038/nclimate2924.

SEA LEVEL

Copernicus Climate Change Service (C3S), 2018: Sea Level Daily Gridded Data from Satellite Observations for the Global Ocean from 1993 to Present. C3S Climate Data Store (CDS), https://doi.org/10.24381/cds.4c328c78.

GMSL from CNES/+, https://www.aviso.altimetry.fr/en/data/products/ocean-indicators-products/mean-sea-level/data-acces.html#c12195.

MARINE HEATWAVE AND MARINE COLD SPELL

Marine heatwaves are categorized as moderate when the sea-surface temperature (SST) is above the ninetieth percentile of the climatological distribution for five days or longer. The subsequent categories are defined in respect of the difference between the SST and the climatological distribution average: "strong", "severe" or "extreme", if that difference is, respectively, more than two, three or four times the difference between the ninetieth percentile and the climatological distribution average.[136]

Marine cold spell categories are analogous but counting days below the tenth percentile, except for the "ice" category. This category is given to any marine cold spell when the threshold for the occurrence on any given day of the event is below –1.7 °C.[137] These are therefore considered to be conditions related to sea ice, and not extreme temperature fluctuations.

The baseline used for marine heatwaves and cold spells is 1982–2011, which is shifted by one year from the standard normal period of 1981–2010 because the first full year of the satellite SST series on which it is based is 1982. This period has not been updated to the current standard normal period of 1991–2020 because the shifting of the baseline has a significant effect on the results and would not allow for comparison of marine heatwaves/marine cold spells statistics with previous versions of the present publication.

All marine heatwaves and cold spells are detected using the NOAA 1/4° Daily Optimum Interpolation Sea Surface Temperature (OISST) v2.1 dataset (Huang et al., 2021).

Hobday, A. J.; Alexander, L. V.; Perkins, S. E. et al. A Hierarchical Approach to Defining Marine Heatwaves. *Progress in Oceanography* **2016**, *141*, 227–238. https://doi.org/10.1016/j.pocean.2015.12.014.

Hobday, A. J.; Oliver, E. C. J.; Sen Gupta, A. et al. Categorizing and Naming Marine Heatwaves. *Oceanography* **2018**, *31* (2), 1–13. https://www.jstor.org/stable/26542662.

Huang, B.; Liu, C.; Banzon, V. et al. Improvements of the Daily Optimum Interpolation Sea Surface Temperature (DOISST) Version 2.1. *Journal of Climate* **2021**, *34 (8)*, 2923–2939. https://doi.org/10.1175/JCLI-D-20-0166.1.

Schlegel, R. W.; Darmaraki, S.; Benthuysen, J. A. et al. Marine Cold-Spells. *Progress in Oceanography* **2021**, *198*, 102684. https://doi.org/10.1016/j.pocean.2021.102684.

ICE SHEETS

Mankoff, K.D.; Fettweis, X.; Langen, P.L. et al. Greenland Ice Sheet Mass Balance from 1840 Through Next Week. *Earth System Science Data* **2021**, *13* (10), 5001–5025. https://doi.org/10.5194/essd-13-5001-2021.

Mankoff, K; Fettweis, X.; Solgaard, A., et al. *Greenland Ice Sheet Mass Balance from 1840 Through Next Week*: GEUS Dataverse, V791, 2021. https://doi.org/10.22008/FK2/OHI23Z.

Gravimetric (Gravity Recovery and Climate Experiment (GRACE)) ice mass time series for the Greenland and Antarctic ice sheets are calculated using spherical harmonics from JPL RL06v1, following Velicogna et al., 2020. The degree-1 geocentre terms are calculated using Sutterley and Velicogna, 2019 using C2,0 and C3,0 coefficients from Loomis et al., 2019. The GRACE/GRACE Follow-on (GRACE-FO) data are corrected for the long-term trend of glacial isostatic adjustment (GIA) from the solid earth using the regional IJ05-R2 GIA model (Ivins et al., 2013) over Antarctica and the regional GIA model over Greenland (Simpson et al., 2009). These regional GIA models do not include realistic GIA signal outside the ice sheets. For this reason, outside Greenland and Antarctica, GIA corrections are based on Geruo et al., 2013 with the ICE6G ice history (Peltier et al., 2015).

Geruo, A.; Wahr, J.; Zhong, S. Computations of the Viscoelastic Response of a 3-D Compressible Earth to Surface Loading: An Application to Glacial Isostatic Adjustment in Antarctica and Canada. *Geophysical Journal International* **2013**, *192* (2), 557–572. https://doi.org/10.1093/gji/ggs030.

Ivins, E.R.; James, T.S.; Wahr, J. et al. Antarctic Contribution to Sea Level Rise Observed by GRACE with Improved GIA Correction. *Journal of Geophysical Research: Solid Earth* **2013**, *118* (6), 3126–3141. https://doi.org/10.1002/jgrb.50208.

Loomis, B.D.; Rachlin, K.E.; Luthcke, S.B. Improved Earth Oblateness Rate Reveals Increased Ice Sheet Losses and Mass-driven Sea Level Rise. *Geophysical Research Letters* **2019**, *46* (12), 6910–6917. https://doi.org/10.1029/2019GL082929.

Peltier, W.R.; Argus, D.F; Drummond, R. Space Geodesy Constrains Ice Age Terminal Deglaciation: The Global ICE-6G_C (VM5a) Model. *Journal of Geophysical Research: Solid Earth* **2015**, *120* (1), 450–487. https://doi.org/10.1002/2014JB011176.

Simpson, M.J.R; Milne, G.A.; Huybrechts, P. et al. Calibrating a Glaciological Model of the Greenland Ice Sheet from the Last Glacial Maximum to Present-day Using Field Observations of Relative Sea Level and Ice Extent. *Quaternary Science Reviews* **2009**, *28* (17–18), 1631–1657. https://doi.org/10.1016/j.quascirev.2009.03.004.

Sutterley, T.C.; Velicogna, I. Improved Estimates of Geocenter Variability from Time-variable Gravity and Ocean Model Outputs. *Remote Sensing* **2019**, *11* (18), 2108. https://doi.org/10.3390/rs11182108.

Velicogna, I.; Mohajerani, Y.; Geruo, A. Continuity of Ice Sheet Mass Loss in Greenland and Antarctica from the GRACE and GRACE Follow-on Missions. *Geophysical Research Letters* **2020**, *47* (8), e2020GL087291. https://doi.org/10.1029/2020GL087291.

GLACIERS

Global glacier monitoring information is provided by the World Glacier Monitoring Service (WGMS):

World Glacier Monitoring Service (WGMS), 2024: *Fluctuations of Glaciers (FoG) Database*, https://doi.org/10.5904/wgms-fog-2024-01.

SEA-ICE

Data are from the *European Organization for the Exploitation of Meteorological Satellites (EUMETSAT) Ocean and Sea Ice Satellite Application Facility Sea Ice Index v2p2*[138] and the National Snow and Ice Data Center (NSIDC) v3 Sea Ice Index.[139] Sea-ice concentrations are estimated from microwave radiances measured from satellites. Extent is the area of ocean grid cells where the sea-ice concentration exceeds 15%. There are modest differences in the absolute extent among datasets, but they agree well on year-to-year changes and trends. In the main text of the present publication, NSIDC values are reported for absolute extents, and rankings. Comparison figures for the Ocean and Sea Ice Satellite Application Facility are given in Table 3 (see below).

Table 3. NSIDC values compared with EUMETSAT Ocean and Sea Ice Satellite Application Facility figures for 2023

Metric	*NSIDC*	*Ocean and Sea Ice Satellite Application Facility*
Arctic daily minimum	4.23 million km², 19 September. Sixth lowest on record.	4.71 million km², 16 September. Sixth lowest on record.
Arctic daily maximum	14.62 million km², 6 March. Fifth lowest on record.	14.64 million km², 3 March
Antarctic daily minimum	1.79 million km², 21 February. Lowest on record.	2.00 million km², 16 February. Lowest on record.
Antarctic daily maximum	16.96 million km², 10 September. Lowest on record.	17.60 million km², 12 September. Lowest on record.

European Organization for the Exploitation of Meteorological Satellites (EUMETSAT) Ocean and Sea Ice Satellite Application Facility, 2023: *Sea-ice Index 1978-onwards, Version 2.2, OSI-420*. EUMETSAT Ocean and Sea Ice Satellite Application Facility, data extracted from Sea-ice index | OSI SAF (eumetsat.int).

Fetterer, F.; Knowles, K.; Meier, W.N. et al. *Sea Ice Index, Version 3*: National Snow and Ice Data Center (NSIDC), 2017. https://nsidc.org/data/G02135/versions/3.

Lavergne, T.; Sørensen, A.M.; Kern, S. et al. Version 2 of the EUMETSAT OSI SAF and ESA CCI Sea-ice Concentration Climate Data Records. *The Cryosphere* **2019**, *13* (1), 49–78. https://doi.org/10.5194/tc-139–2019.

PRECIPITATION

The following Global Precipitation Climatology Centre (GPCC) data sets were used in the analysis:

- First Guess Monthly, https://doi.org/10.5676/DWD_GPCC/FG_M_100
- Monitoring Product (Version 2022), https://doi.org/10.5676/DWD_GPCC/MP_M_V2022_100
- Full Data Monthly (Version 2022), https://doi.org/10.5676/DWD_GPCC/FD_M_V2022_100
- Precipitation Climatology (Version 2022), https://doi.org/10.5676/DWD_GPCC/CLIM_M_V2022_100

In Figure 22, Iceland is shown as being much drier than the long-term average and parts of China as much wetter. This is owing to a change in the way that real-time data are processed and is not reflective of actual conditions.

List of contributors

WMO MEMBERS

Algeria, Andorra, Argentina, Armenia, Australia, Azerbaijan, Bahrain, Barbados, Belgium, Belize, Bosnia and Herzegovina, Brazil, Brunei, Bulgaria, Canada, Chile, China, Croatia, Cyprus, Czechia, Côte d'Ivoire, Denmark, Ecuador, Estonia, Finland, France, Georgia, Germany, Hungary, Iceland, India, Iran (Islamic Republic of), Ireland, Israel, Italy, Japan, Jordan, Kazakhstan, Latvia, Libya, Lithuania, Luxembourg, Malaysia, Mali, Mauritius, Mexico, Morocco, Myanmar, Netherlands (Kingdom of the), New Zealand, Nigeria, Norway, Pakistan, Panama, Paraguay, Peru, Poland, Republic of Korea, Republic of Moldova, Russian Federation, Saudi Arabia, Senegal, Serbia, Singapore, Slovakia, Slovenia, South Africa, Sweden, Switzerland, Syrian Arab Republic, Thailand, Türkiye, Ukraine, United Arab Emirates, United Kingdom of Great Britain and Northern Ireland, United Republic of Tanzania, United States of America, Uruguay, Venezuela (Bolivarian Republic of), Viet Nam.

INDIVIDUAL CONTRIBUTORS

Vicente Anzellini (IDMC), Omar Baddour (WMO), Paul M. Barker (University of New South Wales), Joseph Basconcillo (Philippine Atmospheric, Geophysical and Astronomical Services Administration (PAGASA)), Hamid Bastani (WMO), Jorge Alvar-Beltrán (FAO), Jana Birner (UNHCR), Nicholas Bishop (IOM), Jessica Blunden (NOAA), Roberta Boscolo (WMO), Tim B yer (NOAA NCEI), Anny Cazenave (LEGOS), Xuan Che (UNDRR), Lijing Cheng (Institute of Atmospheric Physics (IAP), Center for Ocean Mega-Science), John Church (University of New South Wales), Damien Desbruyères (IFREMER), Catia Domingues (National Oceanography Centre (NOC)), Robert Dunn (Met Office), Elisabeth du Parc (IOM), Arianna Gialletti (FAO), Giancarlo Pini (WFP), Donata Giglio (University of Colorado Boulder), John E. Gilson (SIO), Alashiya Gordes (FAO), Atsushi Goto (WMO), Sarah Grimes (WMO), Flora Gues (CELAD, Mercator Ocean International), Peer Hechler (WMO), Christopher Hewitt (WMO), Shigeki Hosoda (JAMSTEC), Matthias Huss (ETH Zürich), Amanda Ignatia (UNHCR), Kirsten Isensee (IOC/UNESCO), Piyush Jain (Northern Forestry Centre), Gregory C. Johnson (NOAA PMEL), Christopher Kadow (DKRZ), Hideki Kanamaru (FAO), Maarten Kappelle (UNEP), John Kennedy (WMO), Rachel Killick (Met Office), Brian King (NOC), Nicolas Kolodziejczyk (University of Western Brittany), Animesh Kumar (UNDRR), Mikael Kuusela (Carnegie Mellon University), Gernot Laganda (WFP), Lancelot Leclercq (LEGOS), Yuehua Li (Yunnan University), Ricardo Locarnini (NOAA NCEI), John Lyman (NOAA PMEL), Shawn Marshall (ECCC and University of Calgary), Jesse Mason (WFP), Jutta May (UNDRR), Trevor McDougall (University of New South Wales), Brian Menounos (University of Northern British Columbia), Atsushi Minami (JMA), Audrey Minère (Mercator Ocean International), Oe Mitsuho (JMA), Lev Neretin (FAO), Julien Nicolas (ECMWF), Didier Paolo Monselesan (CSIRO), Sarah Purkey (SIO), James Reagan (NOAA NCEI, University of Maryland), Dean Roemmich (SIO), Sylvain Ponserre (IDMC), Ileana Sinziana Puscas (IOM), Claire Ransom (WMO), David Robinson (Rutgers, The State University of New Jersey), Rogerio Bonifacio (WFP), Kanako Sato (JAMSTEC), Abhishek Savita (GEOMAR), Yousuke Sawa (JMA), Robert Schlegel (University of Paris 1 Panthéon-Sorbonne, National Center for Scientific Research (CNRS), Laboratoire d'Océanographie de Villefranche), Katherina Schoo (IOC/UNESCO), Serhat Sensoy (Turkish State Meteorological Service), Fumi Sezaki (JMA), Jose Álvaro Mendes Pimpao Alves Silva (WMO), Mike Sparrow (WMO/World Climate Research Programme (WCRP)), Johan Stander (WMO), Martin Stendel (Danish Meteorological Institute (DMI)), Toshio Suga (Tohoku University, JAMSTEC), Oksana Tarasova (WMO), Caterina Tassone (WMO/Global Climate Observing System (GCOS)), Blair Trewin (BOM), Thea Turkington (Meteorological Services Singapore/Association

of Southeast Asian Nations (ASEAN) Specialized Meteorological Centre), Isabella Velicogna (University of California), Alex Vermeulen (Integrated Carbon Observation System (ICOS)), Karina von Schuckmann (Mercator Ocean International), Ying Wang (UNEP), Susan E. Wijffels (CSIRO, WHOI), Ahmat Younous Abdel-lathif (WFP), Markus Ziese (DWD, GPCC).

INSTITUTIONS

Australian Bureau of Meteorology (BOM), Australia; Carnegie Mellon University, United States of America; CELAD, France; Center for Ocean Mega-Science, Chinese Academy of Sciences, China; Commonwealth Scientific and Industrial Research Organisation (CSIRO), CSIRO Oceans and Atmosphere, Australia; Cooperative Institute for Satellite Earth Systems Studies (CISESS), United States; Deutsche Klimarechenzentrum (DKRZ), Germany; Deutscher Wetterdienst (DWD), Germany; Environment and Climate Change Canada (ECCC), Canada; ETH Zürich, Switzerland; European Centre for Medium-Range Weather Forecasts (ECMWF), United Kingdom; French Research Institute for Exploitation of the Sea (IFREMER), France; GEOMAR Helmholtz Centre for Ocean Research Kiel, Germany; Global Precipitation Climatology Centre (GPCC), Germany; Hong Kong Observatory (HKO), Hong Kong, China; Institute of Atmospheric Physics, Chinese Academy of Sciences, China; Internal Displacement Monitoring Centre (IDMC), Switzerland; Japan Agency for Marine-Earth Science and Technology (JAMSTEC), Japan; Japan Meteorological Agency (JMA), Japan; Laboratoire d'Océanographie de Villefranche, France; Laboratory for Studies in Spatial Geophysics and Oceanography (LEGOS), France; Mercator Ocean International, France; Met Office, United Kingdom of Great Britain and Northern Ireland; National Oceanic and Atmospheric Administration (NOAA) National Centers for Environmental Information (NCEI), United States; National Oceanography Centre, United Kingdom; NOAA Pacific Marine Environmental Laboratory (PMEL), United States; Northern Forestry Centre, Canadian Forest Service, Natural Resources Canada, Canada; OceanScope, France; Rutgers, The State University of New Jersey, United States; Scripps Institution of Oceanography (SIO), United States; Tohoku University, Japan; Turkish State Meteorological Service, Türkiye; University of Calgary, Canada; University of Colorado Boulder, United States; University of New South Wales, Australia; University of Northern British Columbia, Canada; University of Paris 1 Panthéon-Sorbonne, France; University of Western Brittany, France; Woods Hole Oceanographic Institution (WHOI), United States; Yunnan University, China.

UN AGENCIES

Food and Agriculture Organization of the United Nations (FAO); Intergovernmental Oceanographic Commission (IOC) of the United Nations Educational, Scientific and Cultural Organization (UNESCO); International Organization for Migration (IOM); Office of the United Nations High Commissioner for Refugees (UNHCR); United Nations Environment Programme (UNEP); United Nations Office for Disaster Risk Reduction (UNDRR); World Food Programme (WFP).

Endnotes

[1] Trewin, B.; Cazenave, A.; Howell, S. et al. Headline Indicators for Global Climate Monitoring, *Bulletin of the American Meteorological Society* **2021** *102* (1), E20–E37. https://doi.org/10.1175/BAMS-D-19-0196.1.

[2] World Meteorological Organization (WMO). *Climate Indicators and Sustainable Development: Demonstrating the Interconnections* (WMO-No. 1271). Geneva, 2021.

[3] World Meteorological Organization (WMO). *United in Science 2023*: Sustainable development edition; WMO: Geneva, 2023.

[4] United Nations; Department of Economic and Social Affairs. *Synergy Solutions for a World in Crisis: Tackling Climate and SDG Action Together*; 2023. https://sdgs.un.org/synergy-solutions-world-crisis-tackling-climate-and-sdg-action-together.

[5] Betts, R. A.; Jones, C. D.; Knight, J. R. et al. El Niño and a Record CO_2 Rise. *Nature Clim Change* **2016**, *6* (9), 806–810. https://doi.org/10.1038/nclimate3063.

[6] National Oceanic and Atmospheric Administration (NOAA). *Trends in Atmospheric Carbon Dioxide*. https://gml.noaa.gov/ccgg/trends/mlo.html. Measurements at Mauna Loa were interrupted by a volcanic eruption and the measurement site was temporarily relocated to Maunakea observatories 21 miles to the north.

[7] Commonwealth Scientific and Industrial Research Organisation (CSIRO). *Latest Kennaook / Cape Grim greenhouse gas data. The latest greenhouse gas (GHG) data updated monthly from one of the cleanest air sources in the world*. https://www.csiro.au/greenhouse-gases/.

[8] For anomalies relative to other baselines see Global mean temperature anomalies for 2023 relative to other periods..

[9] Rantanen, M.; Laaksonen, A. The Jump in Global Temperatures in September 2023 Is Extremely Unlikely Due to Internal Climate Variability Alone. *npj Clim Atmos Sci* **2024**, *7* (1), 1–4. https://doi.org/10.1038/s41612-024-00582-9.

[10] Hansen, J.; Sato, M.; Kharecha, P. et al. Earth's Energy Imbalance and Implications. *Atmospheric Chemistry and Physics* **2011**, *11* (24), 13421–13449. https://doi.org/10.5194/acp-11-13421-2011.

[11] von Schuckmann, K.; Palmer, M. D.; Trenberth, K. E. et al. An Imperative to Monitor Earth's Energy Imbalance. *Nature Clim Change* **2016**, *6* (2), 138–144. https://doi.org/10.1038/nclimate2876.

[12] von Schuckmann et al. (2020). Heat stored in the Earth system: where does the energy go? Earth Syst. Sci. Data, 12(3), 2013–2041. https://doi.org/10.5194/essd-12–2013–2020

[13] Cheng, L.; Trenberth, K. E.; Fasullo, J. et al. Improved Estimates of Ocean Heat Content from 1960 to 2015. *Science Advances* **2017**, *3* (3), e1601545. https://doi.org/10.1126/sciadv.1601545.

[14] Intergovernmental Panel on Climate Change (IPCC), 2019: Summary for Policymakers. In: *IPCC Special Report on the Ocean and Cryosphere in a Changing Climate,* https://www.ipcc.ch/site/assets/uploads/sites/3/2022/03/01_SROCC_SPM_FINAL.pdf.

[15] Ocean heat content is measured in zettajoules. A zettajoule is 1 021 joules, which is 1 000 000 000 000 000 000 000 joules.

[16] Cheng, L.; Abraham, J.; Trenberth, K. E. et al. New Record Ocean Temperatures and Related Climate Indicators in 2023. *Adv. Atmos. Sci.* **2024**. https://doi.org/10.1007/s00376-024-3378-5.

[17] von Schuckmann, K.; Minière, A.; Gues, F. et al. Heat Stored in the Earth System 1960–2020: Where Does the Energy Go? *Earth System Science Data* **2023**, *15* (4), 1675–1709. https://doi.org/10.5194/essd-15-1675-2023. Loeb, N. G.; Johnson, G. C.; Thorsen, T. J. et al. Satellite and Ocean Data Reveal Marked Increase in Earth's Heating Rate. *Geophysical Research Letters* **2021**, *48* (13), e2021GL093047. https://doi.org/10.1029/2021GL093047.

[18] Minière, A.; von Schuckmann, K.; Sallée, J.-B. et al. Robust Acceleration of Earth System Heating Observed over the Past Six Decades. *Sci Rep* **2023**, *13* (1), 22975. https://doi.org/10.1038/s41598-023-49353-1.

[19] Minière, A.; von Schuckmann, K.; Sallée, J.-B. et al. Robust Acceleration of Earth System Heating Observed over the Past Six Decades. *Sci Rep* **2023**, *13* (1), 22975. https://doi.org/10.1038/s41598-023-49353-1.

[20] Raghuraman, S. P.; Paynter, D.; Ramaswamy, V. Anthropogenic Forcing and Response Yield Observed Positive Trend in Earth's Energy Imbalance. *Nat Commun* **2021**, *12* (1), 4577. https://doi.org/10.1038/s41467-021-24544-4. Kramer, R. J.; He, H.; Soden, B. J. et al. Observational Evidence of Increasing Global Radiative Forcing. *Geophysical Research Letters* **2021**, *48* (7), e2020GL091585. https://doi.org/10.1029/2020GL091585.

[21] e.g., Loeb, N. G.; Johnson, G. C.; Thorsen, T. J. et al. Satellite and Ocean Data Reveal Marked Increase in Earth's Heating Rate. *Geophysical Research Letters* **2021**, *48* (13), e2021GL093047. https://doi.org/10.1029/2021GL093047. Hakuba, M. Z.; Frederikse, T.; Landerer, F. W. Earth's Energy Imbalance From the Ocean Perspective (2005–2019). *Geophysical Research Letters* **2021**, *48* (16), e2021GL093624. https://doi.org/10.1029/2021GL093624.

[22] Purkey, S. G.; Johnson, G. C. Warming of Global Abyssal and Deep Southern Ocean Waters between the 1990s and 2000s: Contributions to Global Heat and Sea Level Rise Budgets. *Journal of Climate* **2010**, *23* (23), 6336–6351. https://doi.org/10.1175/2010JCLI3682.1.

[23] Cheng, L.; Abraham, J.; Trenberth, K. E. et al. Another Year of Record Heat for the Oceans. *Adv. Atmos. Sci.* **2023**, *40* (6), 963–974. https://doi.org/10.1007/s00376-023-2385-2. Cheng, L.; von Schuckmann, K.; Abraham, J. P. et al. Past and Future Ocean Warming. *Nat Rev Earth Environ* **2022**, *3* (11), 776–794. https://doi.org/10.1038/s43017-022-00345-1.

[24] Changes of these percentages from the provisional report reflect an update to the Cheng et al. dataset, see Cheng, L.; Abraham, J.; Trenberth, K. E. et al. New Record Ocean Temperatures and Related Climate Indicators in 2023. *Adv. Atmos. Sci.* **2024**. https://doi.org/10.1007/s00376-024-3378-5.

[25] Cheng, L.; Trenberth, K. E.; Fasullo, J. et al. Improved Estimates of Ocean Heat Content from 1960 to 2015. *Science Advances* **2017**, *3* (3), e1601545. https://doi.org/10.1126/sciadv.1601545.

[26] Cheng, L.; von Schuckmann, K.; Abraham, J. P. et al. Past and Future Ocean Warming. *Nat Rev Earth Environ* **2022**, *3* (11), 776–794. https://doi.org/10.1038/s43017-022-00345-1.

[27] Smale, D. A.; Wernberg, T.; Oliver, E. C. J. et al. Marine Heatwaves Threaten Global Biodiversity and the Provision of Ecosystem Services. *Nat. Clim. Chang.* **2019**, *9* (4), 306–312. https://doi.org/10.1038/s41558-019-0412-1.

[28] World Meteorological Organization (WMO). *WMO Greenhouse Gas Bulletin – No. 18: The State of Greenhouse Gases in the Atmosphere Based on Global Observations through 2021.* Geneva, 2022.

[29] Friedlingstein, P.; O'Sullivan, M.; Jones, M. W. et al. Global Carbon Budget 2020. E*arth System Science Data* **2020**, *12* (4), 3269–3340. https://doi.org/10.5194/essd-12-3269-2020.

[30] Intergovernmental Panel on Climate Change (IPCC). Climate Change 2023: Synthesis Report. Contribution of Working Groups I, II and III to the Sixth Assessment Report of the Intergovernmental Panel on Climate Change; Core Writing Team, H. Lee and J. Romero, Eds.; IPCC: Geneva, Switzerland, 2023. https://doi.org/10.59327/IPCC/AR6–9789291691647.

[31] Intergovernmental Panel on Climate Change (IPCC), 2021: Climate Change 2021: The Physical Science Basis, Chapter 2, section 2.3.3.5 Ocean pH, https://www.ipcc.ch/report/ar6/wg1/.

[32] Numbers in main text are from National Snow and Ice Data Center (NSIDC). OSI SAF figures are provided in Data sets and methods. https://nsidc.org/arcticseaicenews/2023/03/arctic-sea-ice-maximum-at-fifth-lowest-on-satellite-record/, https://nsidc.org/arcticseaicenews/2023/04/polar-dawn-to-dusk/.

[33] National Snow and Ice Data Center (NSIDC). *Arctic sea ice minimum at sixth lowest extent on record.* https://nsidc.org/arcticseaicenews/2023/09/arctic-sea-ice-minimum-at-sixth/.

[34] Fast December expansion, Arctic Sea Ice News and Analysis (nsidc.org) https://nsidc.org/arcticseaicenews/2024/01/fast-december-expansion/

[35] 1981–2010 is the period used by NSIDC for their monitoring

[36] Liu, J.; Zhu, Z.; Chen, D. Lowest Antarctic Sea Ice Record Broken for the Second Year in a Row. *Ocean-Land-Atmosphere Research* **2023**, *2*, 0007. https://doi.org/10.34133/olar.0007.

[37] Purich, A.; Doddridge, E. W. Record Low Antarctic Sea Ice Coverage Indicates a New Sea Ice State. *Commun Earth Environ* **2023**, *4* (1), 1–9. https://doi.org/10.1038/s43247-023-00961-9.

[38] https://nsidc.org/arcticseaicenews/2023/09/antarctic-sets-a-record-low-maximum-by-wide-margin/.

[39] Fast December expansion, Arctic Sea Ice News and Analysis (nsidc.org) https://nsidc.org/arcticseaicenews/2024/01/fast-december-expansion/.

[40] The period 1981–2010 is used by NSIDC for their monitoring.

[41] Weyer, N. M., Ed. Annex I: Glossary. In IPCC Special Report on the Ocean and Cryosphere in a Changing Climate. Pörtner, H.-O.; Roberts, D. C.; Masson-Delmotte, V. et al., Eds.; Cambridge University Press: Cambridge, UK and New York, USA, 2019. https://www.ipcc.ch/srocc/chapter/glossary/. Note that the Antarctic ice sheet can be further subdivided into West Antarctic, East Antarctic and the Antarctic Peninsula, but is treated here as a single entity.

[42] Note that the Antarctic ice sheet can be further subdivided into West Antarctic, East Antarctic and Antarctic Peninsula, but is treated here as a single entity.

[43] Mankoff, K. D.; Fettweis, X.; Langen, P. L. et al. Greenland Ice Sheet Mass Balance from 1840 through next Week. *Earth System Science Data* **2021**, *13* (10), 5001–5025. https://doi.org/10.5194/essd-13-5001-2021.

[44] National Snow and Ice Data Center (NSIDC). *Late-season melt spike*. https://nsidc.org/ice-sheets-today/analyses/late-season-melt-spike. *Sudden shift to southern heat*. https://nsidc.org/ice-sheets-today/analyses/sudden-shift-southern-heat.

[45] Cumulative melt-day area is the area of the ice sheet that experienced melting conditions each day (diagnosed by the presence of liquid water at the surface), summed over the number of days in the melt season.

[46] Summit Station is the highest point on the Greenland ice sheet, at an altitude of 3 216 m.

[47] https://www.dmi.dk/nyheder/2023/varmerekorder-pa-indlandsisen/

[48] Nghiem, S. V.; Hall, D. K.; Mote, T. L. et al. The Extreme Melt across the Greenland Ice Sheet in 2012. *Geophysical Research Letters* **2012**, *39* (20). https://doi.org/10.1029/2012GL053611.

[49] Otosaka, I. N.; Shepherd, A.; Ivins, E. R. et al. Mass Balance of the Greenland and Antarctic Ice Sheets from 1992 to 2020. *Earth System Science Data* **2023**, *15* (4), 1597–1616. https://doi.org/10.5194/essd-15-1597-2023.

[50] A gigatonne (Gt) is 1 000 000 000 t, and 1 Gt of ice corresponds to a volume of about 1.09 km^3.

[51] m w.e. is the depth of water equivalent to the change in ice thickness. Glacier ice is less dense than water, so the equivalent depth of water is slightly less than the thickness of ice lost.

[52] WGMS (2023): Global Glacier Change Bulletin No. 5 (2020-2021). Michael Zemp, Isabelle Gärtner-Roer, Samuel U. Nussbaumer, Ethan Z. Welty, Inès Dussaillant, and Jacqueline Bannwart (eds.), ISC (WDS) / IUGG (IACS) / UNEP / UNESCO / WMO, World Glacier Monitoring Service, Zurich, Switzerland, 134 pp. Based on database version https://doi.org/10.5904/wgms-fog-2023-09.

[53] Firn is multi-year snow, which has a higher albedo than glacier ice.

[54] LiDAR stands for Light Detection and Ranging, which uses a laser to determine the height of the glacier surface.

[55] Hugonnet, R.; McNabb, R.; Berthier, E. et al. Accelerated Global Glacier Mass Loss in the Early Twenty-First Century. *Nature* **2021**, *592* (7856), 726–731. https://doi.org/10.1038/s41586-021-03436-z.

[56] Parisien, M.-A.; Barber, Q. E.; Flannigan, M. D. et al. Broadleaf Tree Phenology and Springtime Wildfire Occurrence in Boreal Canada. *Global Change Biology* **2023**, *29* (21), 6106–6119. https://doi.org/10.1111/gcb.16820.

[57] Robinson, David A.; Estilow, Thomas W.; and NOAA CDR Program (2012): NOAA Climate Data Record (CDR) of Northern Hemisphere (NH) Snow Cover Extent (SCE), Version 1. NOAA National Centers for Environmental Information. https://doi.org/10.7289/V5N014G9.

[58] IEA (2024), Renewables 2023, IEA, Paris https://www.iea.org/reports/renewables-2023

[59] https://www.cop28.com/en/global-renewables-and-energy-efficiency-pledge

[60] In general, a capacity factor is a measure of how often a power plant operates at its maximum capacity over a certain period, expressed as a percentage.

[61] World Meteorological Organization (WMO), International Renewable Energy Agency (IRENA). 2022 Year in Review: Climate-driven Global Renewable Energy Potential Resources and Energy Demand. Geneva, 2023.

[62] World Meteorological Organization (WMO). *WMO Greenhouse Gas Bulletin – No. 19: The State of Greenhouse Gases in the Atmosphere Based on Global Observations through 2022.* Geneva, 2022.

[63] A Dobson unit is the depth (in units of 10 μm) of the pure gas you would get if it were extracted from the air column and reduced to standard temperature and pressure. 300 DU corresponds to 3mm.

[64] https://ozonewatch.gsfc.nasa.gov/

[65] https://atmosphere.copernicus.eu/monitoring-ozone-layer

[66] https://mausam.imd.gov.in/responsive/monsooninformation.php

[67] United Nations Environment Programme (UNEP). *Frontiers 2022: Noise, Blazes and Mismatches-Emerging Issues of Environmental Concern*. Nairobi, 2022.

[68] Fire weather is weather conducive to wildfires, including high temperatures, low humidity, and high winds.

[69] United Nations, 2022: *The Sustainable Development Goals Report 2022*, https://unstats.un.org/sdgs/report/2022/

[70] United Nations, 2023: *The Sustainable Development Goals Report 2023: Special Edition*, https://unstats.un.org/sdgs/report/2023/.

[71] https://www.mapa.gob.es/es/prensa/ultimas-noticias/el-146--del-territorio-est%C3%A1-en-emergencia-por-escasez-de-agua-y-el-274--en-alerta/tcm:30–659894

[72] https://www.unocha.org/publications/report/libya/libya-flood-response-humanitarian-update-15-december-2023

[73] https://reliefweb.int/report/greece/greece-severe-weather-and-floods-update-greek-civil-protection-hellenic-national-meteorological-service-copernicus-emsr-echo-daily-flash-11-september-2023

[74] https://www.preventionweb.net/media/87994/download?startDownload=true

[75] https://reliefweb.int/report/mozambique/unhcr-mozambique-cyclone-freddy-flash-update-3-24-march-2023

[76] https://story.internal-displacement.org/2023-mid-year-update/

[77] https://sentinel-asia.org/EO/2023/article20230514MM.html

[78] https://reliefweb.int/report/bangladesh/bangladesh-cyclone-mocha-humanitarian-response-situation-report-14-may-2023

[79] National contribution

[80] https://ahacentre.org/wp-content/uploads/2023/05/AHA-DRAFT-Situation_Report-9-TC-MOCHA-Myanmar-1.pdf

[81] https://story.internal-displacement.org/2023-mid-year-update/

[82] https://reporting.unhcr.org/myanmar-emergency-flash-update-2-cyclone-mocha.

[83] https://www.nhc.noaa.gov/data/tcr/EP182023_Otis.pdf

[84] Emergency Events Database (EM-DAT). See also https://www.fitchratings.com/research/insurance/mexico-re-insurers-not-materially-affected-by-hurricane-otis-31-10-2023.

[85] https://reliefweb.int/report/mexico/mexico-hurricane-otis-situation-report-no-01-8-november-2023

[86] https://www.treasury.govt.nz/sites/default/files/2023–04/impacts-from-the-north-island-weather-events.pdf

[87] Merlone, A.; Pasotti, L.; Musacchio, C. et al. Evaluation of the Highest Temperature WMO Region VI Europe (Continental): 48.8°C, Siracusa Sicilia, Italy on August 11, 2021. *International Journal of Climatology* **2024**, *44*, 721–728. https://doi.org/10.1002/joc.8361.

[88] https://meteofrance.com/actualites-et-dossiers/actualites/fortes-chaleurs-aout-2023

[89] https://atmosphere.copernicus.eu/2023-year-intense-global-wildfire-activity

[90] https://www.canada.ca/en/environment-climate-change/services/top-ten-weather-stories/2023.html

[91] https://www.disastercenter.com/FEMA%20Daily%20Ops%20Briefing%20085–2023.pdf

[92] https://www.ncei.noaa.gov/access/billions/events/US/2023?disasters[]=wildfire

[93] https://www.fema.gov/sites/default/files/documents/PDAReport_FEMA4724DRexpedited-HI.pdf

[94] Piyush, J.; Barber, Q.E.; Taylor, S. et al. Canada Under Fire – Drivers and Impacts of the Record-Breaking 2023 Wildfire Season. *Ess Open Archive* **2024**. https://essopenarchive.org/users/747500/articles/719254-canada-under-fire-drivers-and-impacts-of-the-record-breaking-2023-wildfire-season.

[95] https://www.portodemanaus.com.br/?pagina=niveis-maximo-minimo-do-rio-negro

[96] Ethiopia: https://www.unocha.org/publications/report/ethiopia/ethiopia-oct-nov-dec-rainy-season-flash-update-1-18-december-2023. Kenya: https://www.unocha.org/publications/report/kenya/kenya-heavy-rains-and-floods-impact-and-response-20-december-2023. Somalia: https://www.unocha.org/publications/report/somalia/somalia-situation-report-26-dec-2023.

[97] https://dtm.iom.int/reports/east-and-horn-africa-flood-snapshot-july-november-2023

[98] https://dtm.iom.int/reports/horn-africa-drought-human-mobility-snapshot-january-june-2023

[99] National contribution.

[100] https://www.fao.org/3/cc6806en/cc6806en.pdf

[101] United Nations, 2022: *The Sustainable Development Goals Report 2022*, https://unstats.un.org/sdgs/report/2022/.

[102] United Nations, 2023: *The Sustainable Development Goals Report 2023: Special Edition*, https://unstats.un.org/sdgs/report/2023/.

[103] https://docs.wfp.org/api/documents/WFP-0000153758/download/?_ga=2.87190362.312982961.1705667005-702211395.16952869333.

[104] Food and Agriculture Organization of the United Nations (FAO); International Fund for Agricultural Development (IFAD); United Nations Children's Fund (UNICEF) et al., 2023: *The State of Food Security and Nutrition in the World 2023: Urbanization, Agrifood Systems Transformation and Healthy Diets Across the Rural–Urban Continuum*, https://doi.org/10.4060/cc3017en.

[105] docs.wfp.org/api/documents/WFP-0000150404/download/

[106] Food and Agriculture Organization of the United Nations (FAO), 2023: *Crop Prospects and Food Situation – Quarterly Global Report No. 2, July 2023*, https://doi.org/10.4060/cc6806en.

[107] Food and Agriculture Organization of the United Nations (FAO); International Fund for Agricultural Development (IFAD); United Nations Children's Fund (UNICEF) et al., 2023: *The State of Food Security and Nutrition in the World 2023: Urbanization, Agrifood Systems Transformation and Healthy Diets Across the Rural–Urban Continuum*, https://doi.org/10.4060/cc3017en.

[108] Food and Agriculture Organization of the United Nations (FAO), 2021: *The Impact of Disasters and Crises on Agriculture and Food Security: 2021*, https://doi.org/10.4060/cb3673en.

[109] Food and Agriculture Organization of the United Nations (FAO), 2023: *The Impact of Disasters on Agriculture and Food Security 2023: Avoiding and Reducing Losses through Investment in Resilience*, https://doi.org/10.4060/cc7900en.

[110] Food and Agriculture Organization of the United Nations (FAO), 2023: *Crop Prospects and Food Situation – Triannual Global Report No. 3, November 2023*, https://doi.org/10.4060/cc8566en.

[111] Ibid.

[112] World Food Programme (WFP), 2023: *Indonesia – Monitoring Bulletin: July–September (Q3) 2023*, https://www.wfp.org/publications/indonesia-monitoring-bulletin-july-september-q3-2023.

[113] Office for the Coordination of Humanitarian Affairs (OCHA), 2023: *Latin America & The Caribbean Weekly Situation Update (as of 4 September 2023)*, https://reliefweb.int/report/cuba/latin-america-caribbean-weekly-situation-update-4-september-2023.

[114] Food and Agriculture Organization of the United Nations (FAO), 2023: *Crop Prospects and Food Situation – Triannual Global Report No. 3, November 2023*, https://doi.org/10.4060/cc8566en.

[115] https://data-in-emergencies.fao.org/apps/e451e32a054847469b1c1c731a8e5cff/explore

[116] https://www.unhcr.org/news/briefing-notes/un-refugee-agency-warns-extreme-hardship-forcibly-displaced-families-winter

[117] https://go.ifrc.org/emergencies/6435, https://reliefweb.int/disaster/fl-2023-000068-yem

[118] https://dtm.iom.int/reports/migration-along-eastern-corridor-july-2023

[119] https://reliefweb.int/report/pakistan/early-needs-identification-report-monsoon-flood-affected-areas-pakistan-august-2023

[120] https://prmn-somalia.unhcr.org/yearly-displacement

[121] https://reliefweb.int/report/somalia/unhcr-somalia-factsheet-december-2023

[122] https://reliefweb.int/report/libya/libya-impact-storm-daniel-update-displacement-and-needs-november-2023

[123] https://dtm.iom.int/reports/libya-storm-daniel-flash-update-2-13-september-2023

[124] End poverty in all its forms everywhere

[125] End hunger, achieve food security and improved nutrition and promote sustainable agriculture.

[126] Ensure healthy lives and promote well-being for all at all ages.

[127] Reduce inequality within and among countries.

[128] Ensure inclusive and equitable quality education and promote lifelong learning opportunities for all.

[129] Ensure availability and sustainable management of water and sanitation for all.

[130] Ensure access to affordable, reliable, sustainable and modern energy for all.

[131] Achieve gender equality and empower all women and girls.

[132] https://www.unhcr.org/protection/environment/5f21565b4/gender-displacement-and-climate-change.html

[133] United Nations Environment Programme (UNEP), 2022: *Climate Change and Security Partnership Project – Final Report: March 2017–February 2022*, https://wedocs.unep.org/handle/20.500.11822/40549.

[134] https://sendaiframework-mtr.undrr.org/publication/report-midterm-review-implementation-sendai-framework-disaster-risk-reduction-2015–2030

[135] von Schuckmann, K.; Cheng, L.; Palmer, M.D. et al. Heat Stored in the Earth System: Where Does the Energy go? *Earth System Science Data* **2020**, *12* (3), 2013–2041. https://doi.org/10.5194/essd-12-2013-2020.

[136] Hobday, A.J.; Oliver, E.C.J; Gupta, A.S. et al. Categorizing and Naming Marine Heatwaves. *Oceanography* **2018**, *31* (2), 162–173. https://www.jstor.org/stable/26542662.

[137] Schlegel, R.W.; Darmaraki, S.; Benthuysen, J.A. et al. Marine Cold-spells. *Progress in Oceanography* **2021**, *198*, 102684. https://www.sciencedirect.com/science/article/abs/pii/S0079661121001683.

[138] Based on Lavergne, T.; Sørensen, A.M.; Kern, S. et al. Version 2 of the EUMETSAT OSI SAF and ESA CCI Sea-ice Concentration Climate Data Records. *The Cryosphere* **2019**, *13* (1), 49–78. https://doi.org/10.5194/tc-139–2019.

[139] Fetterer, F.; Knowles, K.; Meier, W.N. et al. *Sea Ice Index, Version 3*: National Snow and Ice Data Center (NSIDC), 2017. https://nsidc.org/data/G02135/versions/3.

Food and Agriculture Organization of the United Nations

UNHCR The UN Refugee Agency

IOM UN MIGRATION

WFP World Food Programme

For more information, please contact:

World Meteorological Organization

7 bis, avenue de la Paix – P.O. Box 2300 – CH 1211 Geneva 2 – Switzerland

Strategic Communications Office
Cabinet Office of the Secretary-General

Tel: +41 (0) 22 730 83 14 – Fax: +41 (0) 22 730 80 27

Email: communications@wmo.int

wmo.int

JN 24245